

The competition between endogenous phospholipids and proteins from pea protein isolate rules their interfacial properties

Eléna Keuleyan^a, Jeanne Kergomard^a, Adeline Boire^a, Elisabeth David-Briand^a,
Véronique Vié^{b,c}, Anne Meynier^a, Alain Riaublanc^a, Claire Berton-Carabin^{a,d,*}

^a INRAE, UR BIA, F-44300, Nantes, France

^b Univ Rennes, CNRS, IPR-UMR 6251, Rennes, France

^c Univ Rennes, CNRS, ScanMAT - UAR 2025, F-35042, Rennes, France

^d Wageningen University & Research, Laboratory of Food Process Engineering, 6700 AA, Wageningen, the Netherlands

ABSTRACT

Sustainable incentives foster the use of plant-based ingredients as emulsifiers, but their composition, functionality and interfacial properties deserve more attention. A recent study highlighted high contents of endogenous phospholipids in pea protein isolate (PPI) and the potential of high-pressure homogenization (HPH) to release submicron lipid structures in aqueous suspensions. These findings raised the pivotal question of the interfacial properties of this widespread ingredient, suggesting a competition between proteins and phospholipids for interfacial adsorption. Dilatational interfacial rheology measurements were conducted using either the soluble fraction of the ingredient as such, lipids extracted from PPI, or purified pea proteins (7S). Oscillatory deformations of the oil-water interfacial layers were analyzed using Lissajous plots, which substantiated the interactions between proteins and lipids by deciphering their respective contributions. The formation of mixed interfacial films according to the protein-to-lipid ratio was demonstrated, with a prevalent influence of pea lipids on the rheological signature of the films. Atomic force microscopy confirmed the formation of mixed interfacial films where lipid domains coexist with protein aggregates. These insights advance the current knowledge regarding the complexity and functionality of plant protein ingredients, which is important to promote the rational formulation of plant-based food products.

1. Introduction

In recent years, plant-based ingredients have started to prevail over animal-derived ingredients to stabilize emulsified systems (food, pharmaceuticals, cosmetics, personal care products, etc.) (Loveday, 2019; McClements & Grossmann, 2022). This transition has come along with major challenges as protein-rich ingredients from plants (i.e., protein isolates or protein concentrates) are generally less performant as emulsifiers compared to animal proteins. This is related, at least partly, to their greater structural and compositional complexity (Keuleyan et al., 2023; Moll et al., 2021; Sagis & Yang, 2022). Recently, efforts have been made at enhancing the functionality of pulse protein ingredients, for instance by submitting ingredients' aqueous suspensions to high-shear treatments such as high-pressure homogenization (HPH). This mechanical process uses high pressure to force liquid through a narrow space, thus breaking down particles and droplets. Especially in plant protein isolates, HPH significantly enhances protein solubility (defined as the fraction of proteins that does not sediment under given centrifugation conditions) by altering non-hydrated grain powders and

reducing the size of aggregates (Burger et al., 2021; Grasberger et al., 2022; Keuleyan et al., 2023; Lan Luo et al., 2022; Lijuan Luo et al., 2022; Melchior et al., 2021; Saricaoglu, 2020; Yang et al., 2018). Hence, smaller protein aggregates are more prone to diffuse towards the interface, to adsorb and then to spread, yielding homogenous and thinner interfacial films. (Amagliani & Schmitt, 2017; Yang & Sagis, 2021; Grasberger, Hammershøj, & Corredig, 2023). Moreover, we recently showed that pea and lupin protein ingredients contain a substantial fraction of endogenous lipids, notably phospholipids (Keuleyan et al., 2023). The presence of these polar lipids in protein ingredients raise the question of their role in the interfacial properties of the ingredients. Since the interfacial film protects the formed droplets from flocculation or enhance the resistance against coalescence (Bos & van Vliet, 2001; Walstra, 2003), it is paramount to understand how surface-active component from pulse protein ingredients can stabilize oil-water and air-water interfaces.

When considered individually, proteins and low molecular weight emulsifiers (LMWE; including phospholipids) have well-characterized interfacial properties (Berton-Carabin, Sagis, & Schroën, 2018). Being

* Corresponding author. INRAE, UR BIA, F-44300, Nantes, France

E-mail address: claire.berton-carabin@inrae.fr (C. Berton-Carabin).

<https://doi.org/10.1016/j.foodhyd.2025.111475>

Received 7 January 2025; Received in revised form 3 April 2025; Accepted 22 April 2025

Available online 22 April 2025

0268-005X/© 2025 The Authors. Published by Elsevier Ltd. This is an open access article under the CC BY license (<http://creativecommons.org/licenses/by/4.0/>).

small molecules (typically, from 250 g/mol to ~1200 g/mol), the adsorption behaviour of LMWE is governed by their bulk phase concentration, their free energy, hydrophobically-driven interactions (Weiss, 2005; Bergfreund, Bertsch and Fischer, 2021), and by their lateral mobility (Mackie et al., 1999). While proteins can unfold and rearrange their structural conformation at the interface after adsorption, LMWE do not, nor do they form connected networks (Bos & van Vliet, 2001). Instead, they form compact adsorbed layers (Wilde et al., 2004). LMWE which are dispersible yet not soluble in the bulk phase(s) show a specific phase behaviour as a function of the stress applied upon dilatational deformation of the interface: they are subjected to phase transitions resulting in different physical organizations at the interface (condensed, expanded) (Bos & van Vliet, 2001), or self-assemble in the continuous or dispersed phase (Weiss, 2005). For instance, phospholipids organize themselves as vesicles in water or reverse micelles in oil (Bergfreund et al., 2021). In the case of aqueous suspensions of plant protein ingredients containing endogenous phospholipids, the exact colloidal structure(s) under which phospholipids are present is unknown; it is most likely inherited from the native organization of endogenous lipids in the seeds, the extraction process applied to prepare the protein ingredient, and eventually the HPH treatment.

In simplified model systems, the interfacial properties of mixtures comprising monomeric proteins and LMWE at fluid interfaces has been well described (Maldonado-Valderrama & Patino, 2010; Wilde, 2000). Since they both have completely different adsorption mechanisms and surface activities, competitive processes may be encountered. Such competition may result in a physical destabilization of the emulsion droplets, as the presence of LMWE in protein-stabilized emulsion may weaken the interfacial protein network (Wilde et al., 2004). In addition, specific binding and association between phospholipids and proteins may occur, which can result in peculiar rheological signatures (Bos & van Vliet, 2001). This competition was demonstrated as a function of the LMWE-to-protein molar ratio, both at the oil-water and air-water interface by several authors (Chen, Dickinson, & Iveson, 1993; Clark et al., 1994; Coke et al., 1990; Courthaudon, Dickinson, & Dalgleish, 1991; Waninge et al., 2005), and was proven to be an efficient means for small surface-active molecules to displace large adsorbed ones (Lucassen-Reynders, 1994), in the image of the phenomena named 'orogenic displacement' described by Mackie et al. (1999).

Some authors suggested the potential involvement of endogenous lipids on the interfacial rheological signatures of protein ingredients (mainly for dairy proteins), yet the impact of their presence has hardly been investigated so far (Chen & Sagis, 2019). Systems composed of dipalmitoyl phosphatidylcholine (DPPC), dimyristoyl phosphatidylethanolamine (DMPE), β -lactoglobulin and/or β -casein were studied at the chloroform-water interface by drop tensiometry. The authors concluded on the formation of protein-phospholipid complexes that would display specific surface activity and conformation, different from those of the individual components (He et al., 2008). Other authors highlighted the existence of interactions between purified phospholipids (DPPC) and β -casein at the air-water interface, which were affected by pH (Caro, Niño, & Patino, 2009) and led to structural alterations of the interfacial film (Berton-Carabin et al., 2013). More recently, the complexity of the interfacial properties of a commercial PPI was noticed, relating it to the potential presence of highly surface-active compounds in the ingredient (Grasberger et al., 2022). In the case of rapeseed protein concentrates, the presence of lipids did have an impact on the dilatational rheological response of the formed interfacial film (Yang et al., 2021).

This overview underlines one key research gap to bridge, which is to understand how endogenous phospholipids compete with proteins in plant protein ingredients. Yet, we hypothesize that this phenomenon is very likely to rule the interfacial functionalities of these protein ingredients. This hypothesis becomes even more relevant given that the HPH pre-treatment liberates endogenous lipid assemblies from plant protein ingredient powder grains in the suspension and reduces the size of protein aggregates (Keuleyan et al., 2023).

The aim of this work is to investigate the possible competition between endogenous polar lipids and proteins from a commercial pea protein isolate (PPI) for interfacial adsorption. Its composition was previously thoroughly analyzed (Keuleyan et al., 2023), and a HPH pre-treatment was applied to their total aqueous suspensions. The dilatational rheological properties of the interfacial films formed at the oil-water interfaces were examined. We used Lissajous plots, which represent the change in surface pressure as a function of the applied deformation (Sagis & Fischer, 2014; Sagis & Scholten, 2014), to capture complex interfacial behaviours, at different concentrations. Next, we dug deeper into the individual contributions of proteins and polar lipids to the interfacial behaviour at the oil-water interface. For this, we studied a purified mix of vicilins and convicilins (7S proteins) from pea, a dispersion of endogenous lipids extracted from PPI, and combinations thereof in various protein-to-lipid ratios. Finally, further analyses of the air-water interface were performed using a Langmuir trough, by tensiometry and ellipsometry, before being transferred on mica (Langmuir-Blodgett technique) for subsequent microstructure imaging by atomic force microscopy (AFM).

2. Materials and methods

2.1. Reagents and samples

Phosphate dibasic heptahydrate (CAS number: 7782-85-6), sodium phosphate monobasic (13472-35-0) were from Sigma Aldrich (St Louis, USA). Sodium chloride (7647-14-5) was from VWR International (Radnor, USA). Chloroform and methanol were from Biosolve Chemicals (Dieuze, France). All the reagents were of analytical grade, and ultrapure water was used. Commercial rapeseed oil was purchased in a local supermarket.

Pea protein isolate (PPI, ref. S85F) was kindly donated by a commercial provider (Roquette, Lestrem, France). To decipher the interfacial properties of proteins vs lipids from pea, a purified extract of 7S pea proteins was used. These globulins (globular proteins), namely vicilins and convicilins, have an approximate molecular weight of 150–210 kDa (Drusch, Klost, & Kieserling, 2021; Yang & Sagis, 2021). The relative proportions of 7S proteins in the soluble phase of PPI appeared to be less affected by HPH than 11S legumins (Keuleyan et al., 2023), and pea vicilins were shown to have better emulsifying properties than their legumins counterparts (Dagorn-Scaviner, Gueguen and Lefebvre, 1987), which is why they were chosen for this study. A batch of 7S protein was purified from pea flour (Sotexpro) using an adapted protocol, published previously (Larré & Gueguen, 1986). The crude protein extract was prepared by stirring pea flour with 50 mM Tris buffer (pH 8.0) for 4 h at room temperature with a solid:liquid ratio of 1 g: 10 mL. The resulting slurry was centrifuged at 10,000 rpm for 25 min. The procedure was repeated twice to recover most of soluble proteins. Supernatant were combined and injected on an anion exchange chromatography (DEAE streamline column, GE Healthcare, 260 mL). The elution of 7S protein was performed using a step-wise gradient of increasing NaCl (50 mM Tris buffer, 500 mM NaCl, pH 8.0). The eluted fractions were pooled, desalted on a Cellufine GH 25 column (JNC Corporation, 7.5 L, equilibrated in 1 g/L sodium carbonate buffer) and freeze-dried. The protein was further purified by gel filtration on a Cellufine GCL 2000HF column (JNC Corporation, XK50/100, 1.8 L) equilibrated in phosphate buffer (0.1M, pH 7.5). Finally, the samples were dialyzed against sodium carbonate buffer (1 g/L) before freeze-drying.

2.2. Sample preparation and characterization

2.2.1. Preparation of the soluble fractions from HPH-treated suspensions

Since the PPI powder was poorly hydrated after overnight stirring, PPI suspensions were subjected to HPH as previously detailed (Keuleyan et al., 2023) to ensure good dispersion and to enhance the reproducibility of the experiments. Briefly, aqueous suspensions (10 g proteins/L,

in 10 mM phosphate buffer with 90 mM NaCl, pH 7.0) were hydrated under magnetic stirring for 2 h before being homogenized (300 bars, 3 min) using a high-pressure homogenizer (Panda plus 1000, GEA Niro Soavi, Italy).

Only the so-called soluble fraction of this suspension (i.e., the fraction that remains in suspension after centrifugation) was used for further experiments, to prevent bias induced by non-soluble material. To obtain this soluble fraction, HPH-treated suspensions were centrifuged ($20,000\times g$; 30 min; 4 °C; Sigma 3K15, Thermofisher) in 2-mL tubes. An upper-creamed phase was carefully removed using a glass pipette, as illustrated in Fig. 1, and the soluble fraction beneath this creamed phase was recovered. The protein content of this soluble phase was determined with the Dumas combustion analysis method (Elementar, Langensfeld, Germany) (method reference ISO/TS 16634–2:2009), and a nitrogen-to-protein conversion factor of 5.7 was used (Keuleyan et al., 2023). Then, the soluble fractions were diluted in buffer at 0.01 g/L; 0.1 g/L and 1 g proteins/L. The solutions were preserved by adding sodium

azide at 0.02 wt% and stored at +4 °C during one week maximum. Independent duplicates of HPH-treated suspensions were prepared.

2.2.2. Preparation of endogenous lipid dispersions from the soluble fraction of PPI

Lipid extraction. Total lipids from PPI powder were previously quantified (Keuleyan et al., 2023). However, since the soluble fraction of the HPH-treated aqueous suspensions was used in the present study, it was necessary to quantify endogenous lipids from this specific fraction. Lipids of the soluble fraction of PPI were retrieved by chloroform/methanol extraction after some modifications (Folch, Lees, & Sloane Stanley, 1957; Bligh & Dyer, 1959). After the HPH treatment, 100 mL of suspension (10 g proteins/L) were centrifuged in 50-mL tubes at $20,000\times g$ for 1 h at 10 °C (Avanti J-265 XP, Beckman Coulter, Brea, USA). Around 20 g of supernatant were placed in pre-weighed 50-mL Falcon tubes and put in a rotative evaporator (using the aqueous method of Genevac EZ-2.3, SP Scientific, Warminster, UK) under reduce

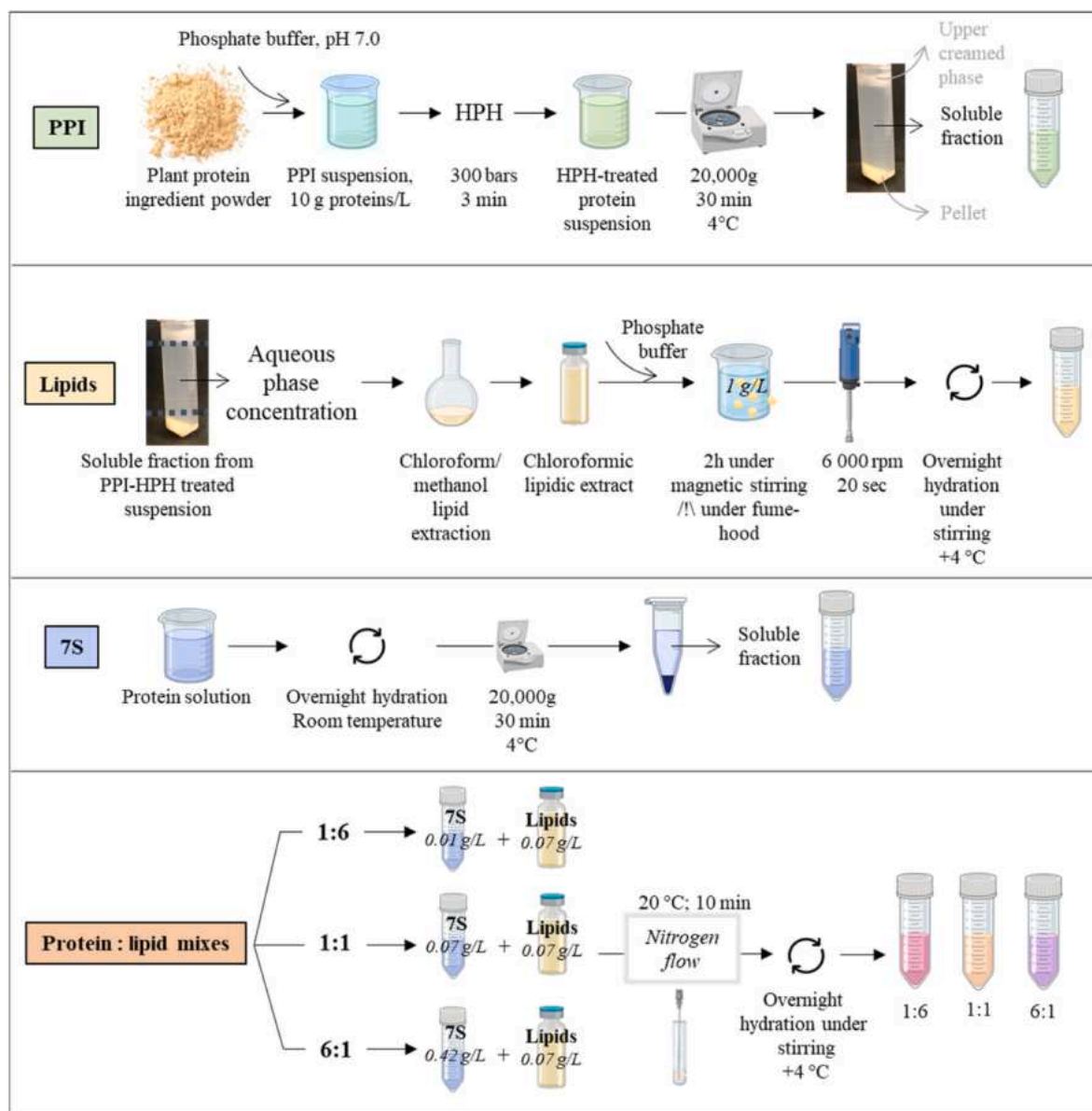


Fig. 1. Schematic representation of the experimental design and the preparation of the samples. Row 1: PPI, treated by HPH (300 bars, 3 min). The same treatment was applied for all the plant protein ingredients of the study. The soluble fraction was collected and diluted. Row 2: this soluble fraction was also used for lipid extraction. This extract was then used to create the lipid dispersion, using a rotor-stator homogenizer. Row 3: a solution of purified pea proteins (7S) was prepared, after hydration and centrifugation. Row 4: mixes of purified proteins with dispersed lipids were prepared as model systems.

pressure for 6 h in order to concentrate the aqueous phase. The concentrated fractions were weighed, and about 12 g of concentrated supernatant were used for lipid extraction and were transferred in 500-mL separating funnel. The appropriate volume of chloroform/methanol (2:1) was prepared for each sample to reach a ratio of 1:20 as sample-to-solvents (Folch et al., 1957). Then, the tubes were rinsed and vortexed three times with the solvent mix before being transferred into the separating funnel. A solution of NaCl (0.73 % w/v) was added to enhance phase separation, up to 25 wt% of the total volume of sample/solvent. The separating funnels were shaken, and let to phase separate at 4 °C for 6 h. Then, the bottom organic phase was recovered in pre-weighed 500-mL spherical flasks, and the separating funnels were washed with 2 x 100 mL of chloroform. The solvent was evaporated under vacuum in a water bath (40 °C) (R-100, Rotavapor, Büchi, France), and dried under nitrogen flow (N-evap 111, Organomation, USA) for 1 h. The lipids were weighed, before being re-solubilized in chloroform to a concentration of 2–3 mg/mL, and stored at –80 °C. Lipid extractions were carried out on three independent HPH-treated soluble fractions from PPI.

Lipid identification. To identify and quantify the lipid classes from this extract, an analysis by U-HPLC (Ultimate 3000 RSLC (Dionex, France) equipped with an evaporative light scattering detector (ELSD, Sedex 85) and an analytical column packed with a silica normal-phase (Uptisphere CS Evolution SI: 150 mm × 4.6 mm, 2.6 µm (Interchim, Montluçon, France)) was performed. A linear gradient of chloroform (eluent A) and mix of CH₃OH/CHCl₃/NH₄OH (460/5/35; v/v/v) (eluent B) was set to allow the chromatographic separation of lipid classes (t_0 : 0 % B, $t_{8 \text{ min}}$: 50 % B, $t_{12 \text{ min}}$: 100 % B, and isocratic conditions with 100 % B for 3 min). The quantification was enabled by a calibration curve made with commercial standards as described before (Keuleyan et al., 2023).

Lipid dispersion preparation. The lipid extract from the soluble fraction of PPI was used to prepare a dispersion of endogenous lipids (Fig. 1). An aliquot of the lipid extract was taken to reach a concentration of 1 g of lipids/L and was poured into 15 mL of buffer and stirred under strong magnetic agitation for 2 h under the fumehood to allow chloroform complete evaporation. Then, a rotor-stator homogenizer was used to disperse the lipids (6000 rpm; 20 s; stator diameter 12 mm; Silent Crusher M, Heidolph, Schwabach, Germany), before overnight hydration under magnetic stirring (4 °C). Dilutions at 0.01 g lipids/L; 0.05 g/L and 0.07 g/L were prepared and added with sodium azide (0.02 wt %) for a maximum storage duration of a week (further details about the concentrations are given in section 2.3.1). Dynamic light scattering analyses were conducted on this dispersion to measure the sizes of the lipid assemblies generated, and the results are provided in [Supplementary Information 1](#). Independent duplicates were carried out.

2.2.3. Preparation of purified 7S pea protein solution

A solution of purified 7S at 3 mg/mL was hydrated overnight in phosphate buffer at room temperature. Then, the solution was centrifuged (20,000×g; 30 min; 4 °C; 2 mL tubes) (Sigma 4K15, Thermofisher) and the supernatant was set aside for further dilutions. Beforehand, protein solubility was determined as previously described (Keuleyan et al., 2023), leading to 79 wt% of soluble proteins. Based on this result, 7S pea proteins solutions were prepared at 0.01 g proteins/L; 0.1 g/L and 1 g/L (Fig. 1). Sodium azide (0.02 wt%) was added and the solutions were stored at 4 °C for a maximum duration of a week. Independent duplicates were performed.

2.2.4. Preparation of the model systems: aqueous mixtures of purified proteins and endogenous lipids

Purified 7S pea protein solutions (2 mL) were prepared at the targeted concentrations (0.01 g/L; 0.07 g/L and 0.42 g/L) in 10 mL glass tubes, as described in section 2.2.3. Then, the corresponding amounts of lipid extract in chloroform, from the soluble fraction of PPI, were added to reach the targeted lipid concentration of 0.07 g/L. Chloroform was evaporated through nitrogen flow using a PuriVap-6 (Interchim,

Montluçon, France) (dry bath at 20 °C) (Fig. 1). Contrary to the procedure applied for lipids only, no additional mechanical dispersion was applied. The dispersions were left under stirring at 4 °C overnight. The solutions were added with sodium azide (0.02 wt%) for a maximum storage of one week, in independent duplicates.

2.3. Dilatational rheology at the oil-water interface

2.3.1. Interfacial tension measurement

Rapeseed oil purification was conducted prior to drop tensiometry analyses. It was performed with magnesium silicate powder (Florisil, Supelco, 100–200 mesh, CAS: 1343-88-0). This procedure allows to remove surface-active impurities while preserving endogenous tocopherols (Berton-Carabin, Ribourg-Birault, & Benatti Gallo, 2024). Purified oil aliquots were stored at –80 °C for maximum six months of storage.

The interfacial tension was measured using an automated drop tensiometer (Tracker, Teclis Instruments, Civrieux d'Azergues, France). Briefly, a pending drop of aqueous solution is created at the tip of a motor-controlled G-18 needle, in a cuvette filled of purified rapeseed oil. This configuration was chosen to avoid problem with turbidity in the soluble protein solution. The shape of the drop is monitored by a camera, thanks to which the interfacial tension is calculated by fitting with the Young-Laplace equation. The experimental set up is illustrated in Fig. 2, along with the summary of the aqueous phases and their concentrations used in this study. A water bath maintained the temperature of both the cuvette and the syringe at 24 °C. A syringe of 500 µL (SGE syringe, Supelco, Bellefonte USA) was used to generate a drop with constant surface area of 13 mm², 30 mm² or 38 mm² depending on the sample and concentration. A 18-Gauge needle (internal diameter: 0.84 mm, length: 100 mm) was used for all samples. The change in surface area was necessary to reach a satisfying Bond number (>0.1) at the beginning of the oscillatory deformations, and because some samples had too low interfacial tension to prevent the drop from pulling away during the experiment. The concentrations of the lipid dispersion were chosen to align with PPI regarding the maximum amount of lipids per interfacial area (mg lipids/mm²).

Each sample was first stabilized for 3 h (waiting time) before launching sinusoidal dilatational deformations, i.e., extension and compression cycles. Three strain sweeps were performed, with surface deformations of 3.3, 5 and 10 % when the drop had a surface area of 13 mm²; or 10, 20 or 30 % for drops with surface areas of 30 mm² or more. The oscillation frequency was 0.02 Hz. For each amplitude variation, five oscillation cycles (250 s) were carried out, followed by 250 s of pause before the next oscillation cycle. Three independent replicates were conducted for each sample and each concentration. Frequency sweeps were also performed at 0.01, 0.02 and 0.05 Hz and at fixed surface deformations of 3.3 %. The results of elastic and loss moduli are provided in [Supplementary Information 2](#).

The interfacial tension between purified oil and ultrapure water ($\gamma_{\text{oil-water}}$) was measured before each series of experiments (ranging between 28.2 mN/m and 31 mN/m). It was used for surface pressure calculations (π , expressed in mN/m) as a function of log (time) (Equation (1)).

$$\pi(t) = \gamma_{\text{oil-water}} - \gamma(t) \quad \text{Equation 1}$$

2.3.2. Data analysis as Lissajous plots

Large amplitude deformations allow to observe non-linearities in the rheological behaviour of interfacial films, which may be relevant for the mechanisms of emulsion destabilization and coalescence (Dickinson, Murray, & Stainsby, 1988; Botti et al., 2022). To characterize non-linear responses, raw data can be represented as Lissajous curves, where the surface pressure ($\gamma(t) - \gamma_0$) (mN/m) is plotted as a function of the amplitude of the deformation $\frac{A(t) - A_0}{A_0}$ (%); where γ_0 corresponds to the interfacial tension at the beginning of the oscillations (mN/m); $A(t)$ is the area of the drop (mm²) at a given time; and A_0 is the area of the

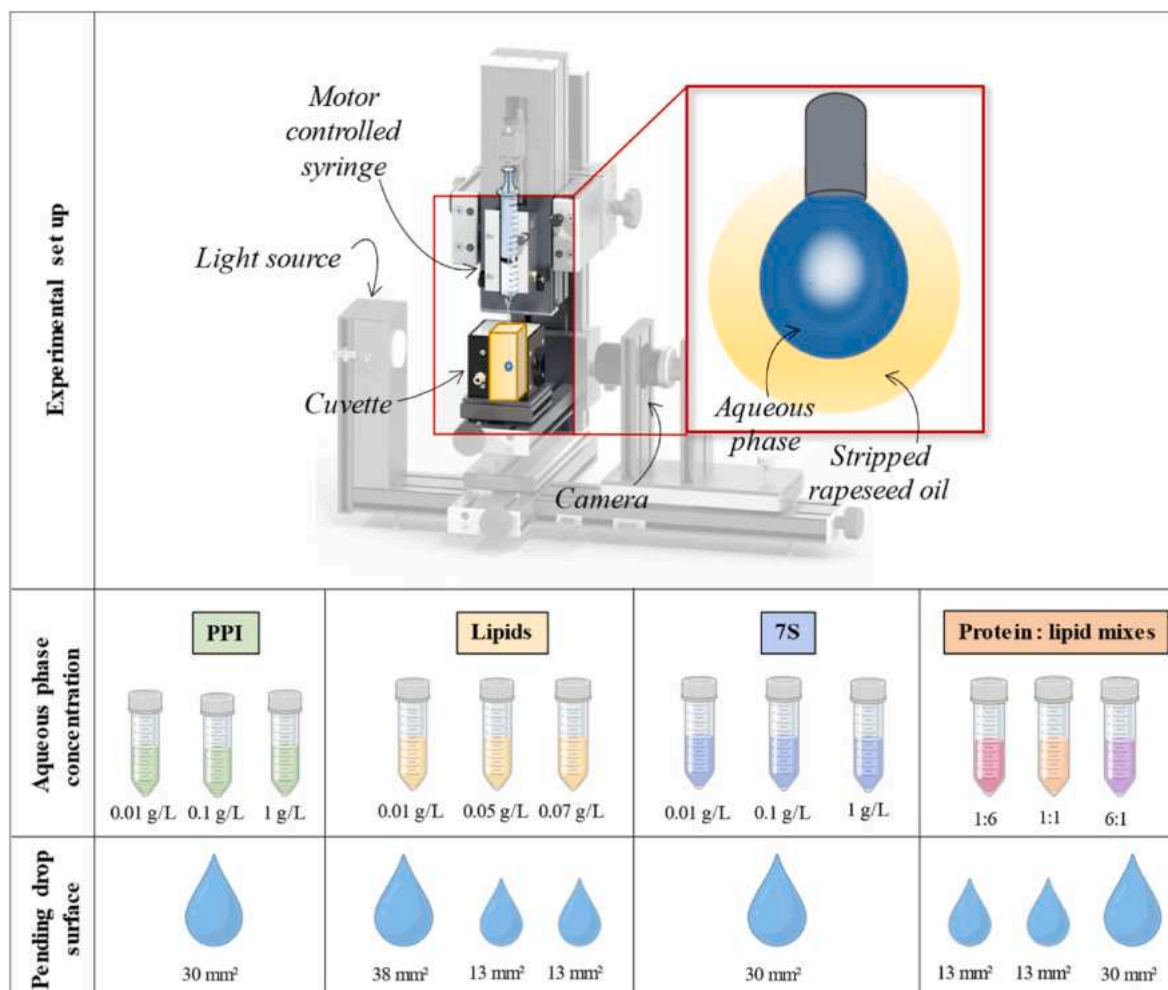


Fig. 2. Experimental design of interfacial tension measurements. Row 1: the set up consists in a pending drop of aqueous phase in an environment of stripped rapeseed oil. Row 2: the different aqueous phases used in this work are given along with their concentrations for PPI, lipid dispersion, 7S protein solution, and protein-to-lipid mixes (from left to right). Row 3: surface of the pending drop according to the sample (mm²). The image of TRACKER™ Standard Drop Tensiometer was taken from www.teclis-scientific.com (February 2024).

non-deformed interface (mm²). The software R (4.2.2) was used to process the data and generate the plots, with the RStudio interface (2022.12.0 + 353). Multiple packages were used (tidyverse, dbplyr, readxl, ggplot2, svglite, viridis, ggh4x, shades, ggtext, cowplot, RColorBrewer, grDevices). The script can be made available upon request.

2.4. Structural characterization of interfacial films at the air-water interface

In order to gain in-depth information regarding the impact of the composition and lipid-to-protein ratio on the interfacial behaviour and organization, selected samples were also studied at the air-water interface using several devices as further detailed in this section. Two distinct soluble fractions from PPI (HPH-treated, cf. section 2.2.1) were prepared, at a final concentration of 0.01 and 1 g/L, respectively. Model systems of 7S pea and PPI endogenous lipid were also probed, at a final concentration of 0.1 and 0.07 g/L, respectively. Those concentrations were chosen based on the drop tensiometry outcomes at intermediate or maximum concentrations.

2.4.1. Ellipsometry and surface pressure measurements

Control ellipsometric and tensiometric measurements were performed for 30 min on 10 mM phosphate buffer (pH 7.0) prior to the experiments to check the cleanliness of the surface. Surface pressure (π)

was measured every 4 s with a precision of ± 0.2 mN/m using a filter paper connected to a microelectronic feedback system (Nima Technology, UK), according to the Wilhelmy plate method. The ellipsometric angle (Δ) was recorded simultaneously every 4 s with a precision of $\pm 0.5^\circ$, using a home-made automated ellipsometer in a “null ellipsometer” configuration (Berge & Renault, 1993; Bourlieu et al., 2020). The laser beam probed a surface of 1 mm² and a depth of 1 μ m, providing insights into the thickness of the interfacial film. Surface pressure monitoring allows to obtain information about the lateral interactions between the amphiphilic molecules at the air-water interface, whereas ellipsometry measurements based on the change in polarization of a reflected light, provide insights into the thickness and refractive index of the films (Azzam, Bashara, & Balard, 1978; Nylander, Hamraoui, & Paulsson, 1999), thus offering the opportunity to study the film formation and evolution throughout the adsorption of the amphiphilic molecules (Azzam et al., 1978; Russev, Arguirov, & Gurkov, 2000).

2.4.2. Preparation of Langmuir-Blodgett films

Before each experiment, the Teflon trough was carefully cleaned with ultrapure water and ethanol to get rid of surface-active impurities. Then, 50 mL of the samples were poured in a computer-controlled and user-programmable Langmuir-Blodgett Teflon Langmuir trough (KSV Nima, Helsinki, Finland) with a surface area of 45 cm² fitted with two mobile barriers. The formation of Langmuir films at the air-water

interface was then monitored for each system for 3 h until the stabilization of the surface pressure, as carried out in drop tensiometry analyses. The interfacial films were transferred onto a freshly-cleaved mica plate using the Langmuir-Blodgett method at a constant surface pressure according to the sample (18.2 mN/m for 7S and PPI (0.01 g/L) or 30 mN/m for lipids and PPI (1 g/L)) and at a very low speed (0.5 mm/min). For each Langmuir film, kinetic measurements were performed in duplicate.

2.4.3. Atomic force microscopy imaging

Imaging was carried out with an AFM (Multimode Nanoscope 5, Bruker, France) in contact mode QNM in air (20 °C), using a standard silicon cantilever (0.06 N/m, SNL-10, Bruker, France), and at a scan rate of 1 Hz. The force was minimized during all scans and the scanner size was $100 \times 100 \mu\text{m}^2$. The processed images analyzed by the open-source platform Gwyddion are representative of at least duplicated experiments and on two different zones on each sample.

3. Results and discussion

3.1. Behaviour of PPI at the oil-water interface

Our previous work showed that PPI powder contains a substantial amount of lipids, accounting for $11.7 \pm 0.4 \text{ wt\%}$ (d.m.) (Keuleyan et al., 2023). Here, we also measured the amount and the composition of lipids remaining in the soluble fraction of the aqueous PPI suspension. After optimization of the lipid extraction methodology for such a diluted phase, we determined that the soluble fraction of PPI contained $0.86 \pm 0.02 \text{ mg lipids/g supernatant}$. This corresponds to a protein-to-lipid mass ratio of 6:1 in the soluble fraction which is close to that measured in the total suspension (6.4). The composition of these extracted lipids was fairly similar to those present in the total powder, with 64 wt% of polar lipids (phosphatidylcholine, phosphatidylinositol and phosphatidylethanolamine), and 36 wt% of triglycerides. This result suggests that there is no preferential partitioning of the different lipid classes among the total suspension and the soluble phase obtained after centrifugation.

These outcomes imply that the soluble fraction contains both endogenous polar lipids and proteins. Their respective roles and interactions regarding the overall interfacial properties of the samples is a major research question that has not been addressed so far, and that we aimed to investigate.

3.1.1. Adsorption kinetics

The change in surface pressure over time was monitored for the soluble fractions of PPI at three different protein concentrations: 0.01 g/L; 0.1 g/L and 1 g/L by pending drop tensiometry (Fig. 3). At the lowest

concentration, surface pressure remained stable and close to 0 until 100 s. It then increased until around 11 mN/m. When increasing the protein concentration by a 10-fold factor (0.1 g/L), the initially measured surface pressure was around 4 mN/m, then rose to 16 mN/m. Those values are slightly higher than some existing values found in the literature (around 10–12 mN/m) (Chang et al., 2015; Kontogiorgos & Prakash, 2023); this could be related to the fact that in the present work, the suspensions were treated by HPH which largely affects the colloidal organization, or to the widely used nitrogen-to-protein conversion factor 6.25 in the literature that leads to an overestimated protein concentration (Keuleyan et al., 2023). At 1 g/L, surface-active molecules readily adsorbed at the interface during the drop formation phase, leading to an initial surface pressure around 12 mN/m, which further increased to around 16 mN/m after 3 h.

These results are consistent with the known mechanisms of adsorption for proteins which are governed by a logarithmic time-dependence diffusion rate towards the oil-water interface (Beverung et al., 1999). The change in surface pressure becomes noticeable when enough material reaches the interface: it is described as the induction regime (I), as observed until 100 s for the most diluted samples, where the surface pressure is not showing noticeable increase. Proteins and other surface-active molecules then accumulate and start to rearrange to induce an increase in the slope of the surface pressure adsorption curve, where the second regime begins. It is characterized as the monolayer saturation, where adsorbed proteins unfold and rearrange, possibly losing part of their secondary or tertiary structure (Renault et al., 2002; Sagis & Yang, 2022). In this regime and the third one, newly materials from the bulk may still diffuse towards the interface and adsorb, thus possibly leading to protein aggregation and increasing film thickness. Then the third regime, interfacial gelation, is identified as a pseudo-plateau. The conformational rearrangement of proteins at the interface aims at reaching the lowest free energy between the oil and water phases (Vasilakis & Doxastakis, 1999): strong in-plane interactions are likely to occur. Yet, rearrangements at the interface is an ongoing process, which is why an equilibrium state cannot be achieved within only a few hours.

With the increase of bulk protein concentration, the disappearance of the induction and rearrangement period is observed, and was already described for other plant proteins, leading some authors to build master curves of adsorption (Kontogiorgos & Prakash, 2023; Poirier et al., 2021). Recent research found similar surface pressure end-values at 0.01 % proteins of a commercially homogenized PPI in close experimental set up (Grasberger et al., 2024). It is important to underline the importance of the colloidal state of the materials present in the bulk on their interfacial properties. In plant protein ingredients, multiple colloidal states are expected to be present in the non-sedimented fraction referred to as the ‘soluble’ phase (Schmitt et al., 2021). Finally, with

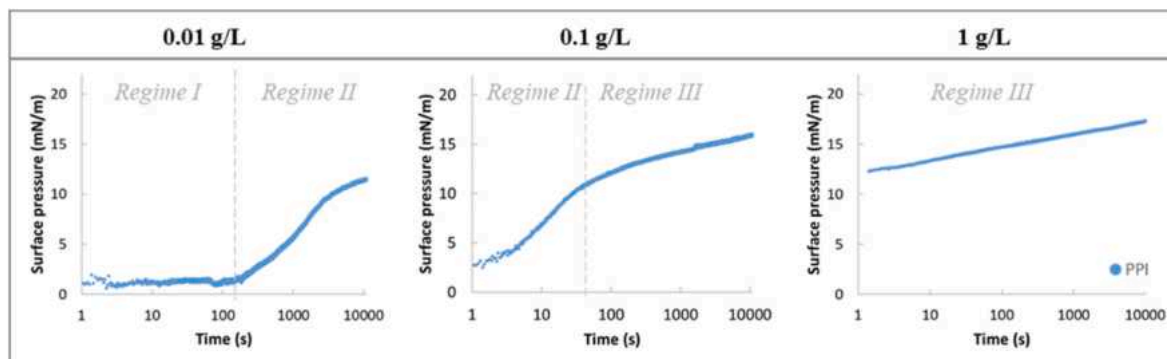


Fig. 3. Surface pressure (mN/m) as a function of time (s), representing the adsorption kinetics at the oil-water interface of the soluble fractions of PPI. Three different protein concentrations were probed (0.01 g/L; 0.1 g/L; 1 g/L; from left to right). The classical adsorption regimes described by Beverung, Radke, & Blanch, 1999 were identified by changes in slope (I (induction), II (rearrangement, monolayer saturation) or III (interfacial conformational changes, gelation)). Experiments were performed in independent triplicates, and representative curves are provided here.

complex protein sources such as PPI, interfacial tension kinetics may not be solely attributed to the adsorption of proteins, as the contribution of highly surface-active minor compounds can be significant (Grasberger et al., 2022, 2024).

3.1.2. Behaviour of the interfacial films under oscillatory dilatational deformation

Emulsions are often subjected to shear or dilatational deformations during processing or destabilization. For example, the onset of droplet coalescence involves large dilatational deformation of the interface, which can be assessed by performing oscillatory dilatational amplitude sweeps in a drop tensiometer (Chen & Sagis, 2019). In the present work, this was conducted after 3 h of aging of the interfacial films from the soluble fractions of PPI at 0.01 g/L, 0.1 g/L and 1 g/L. As dilatational moduli are extracted from the first harmonic of the Fourier transformed signal, first harmonic moduli are meaningless when the response is nonlinear, which are often implied during large deformations (Sagis & Fischer, 2014; Sagis & Scholten, 2014; Sagis, Humblet-Hua, & Van Kempen, 2014). For completeness, interfacial modulus, dilatational elastic moduli and dilatational loss moduli are provided in [Supplementary Information 3](#). Nevertheless, results were mostly analyzed as Lissajous curves, i.e., showing the surface pressure variation as a function of the applied drop surface deformation ([Fig. 4](#)). A concentration dependency of the interfacial rheological behaviour was observed. At 0.01 g/L, a linear elastic behaviour was observed, typical of interfacial films covered with proteins. When increasing protein concentration, non-linearities appeared, as Lissajous curves tended to be more and more asymmetric. This observation is particularly pronounced at 1 g/L, with the formation of viscoelastic films displaying strain softening in extension and strain hardening in compression, indicative of complex interfacial microstructure and soft glass-like behaviour (Sagis & Scholten, 2014). The viscous contribution increased (more opened ellipse shape), with a strain softening behaviour in extension (upper part of the curve), pointing to a disruption of the interfacial microstructure (Sagis & Yang, 2022; Yang et al., 2023). The strain hardening behaviour in compression (lower part of curve) suggests a propensity of the interfacial film to form a dense and compact structure that resists deformation. Moreover, the increase of the viscous contribution with the bulk concentrations was previously well recognized, and described as resulting from a saturation of the interface monolayer (Graham & Phillips, 1980; Vasilakis & Doxastakis, 1999). This increase might also witness that adsorbed molecules self-assemble into microstructures, leading to thicken the interface (Sagis & Scholten, 2014).

Lissajous curves are useful to probe differences in the molecules composing the interfacial films and in their in-plane interactions.

Similar responses to large deformations at the oil-water interface were reported for pea (soluble fraction of PPI – yet not treated by HPH (Hinderink et al., 2020; Shen, Li, & et al, 2023)). In the present work, a specific feature is the compositional complexity of the samples (comprising both proteins and endogenous lipids). Therefore, it is very likely that the increase in bulk concentration enhances the competition between proteins and phospholipids for adsorption at the interface, which could explain the strong concentration effect on the obtained profiles. This is in line with the findings of Yang et al. (2021) who reported the formation of a less stiff and more stretchable interfacial film when the concentration of non-defatted rapeseed protein concentrate was increased, which was hypothesized to be due to non-protein components. To further understand the contributions of these individual components, the next part will deepen their respective interfacial properties.

3.2. Behaviour of purified components (proteins and lipids) at the oil-water interface

3.2.1. Adsorption kinetics

The interfacial properties of purified pea vicilins and convicilins (7S) were evaluated at the oil-water interface at three concentrations: 0.01 g/L; 0.1 g/L and 1 g/L, following the same methodology as previously described. A dispersion of PPI endogenous lipids in phosphate buffer was used to assess the interfacial rheological properties of the formed lipid-based films. Three concentrations were probed: 0.01 g lipids/L, 0.05 g/L and 0.07 g/L. Lipids were dispersed in phosphate buffer (pH 7.0) using a rotor-stator homogenizer, to be consistent with the situation for protein ingredient samples, in which both lipids and proteins are dispersed in the aqueous phase.

Adsorption kinetics of 7S pea proteins are presented in [Fig. 5A](#). A concentration dependency of the relative increase in surface pressure was observed, in the same range as that observed for PPI ([Fig. 3](#)). At low concentration (0.01 g/L), the induction period lasts about 100 s, after which surface pressure begins to increase. At 0.1 g/L, the exponential rise during interfacial saturation is clearly visible. At 1 g/L, the first measurement points are already around 7 mN/m, suggesting a very fast adsorption of small proteinaceous compounds at the interface. In a previous study, it was shown that the stabilization of emulsion droplets (10 wt% oil) with purified pea fractions was mostly enabled by small pea protein molecules (size range of 4 nm radius), at the expense of larger pea protein aggregates (particles) of 60 nm radius (Sridharan et al., 2020). These large structures diffuse more slowly to the interface, then adsorb and unfold, and can self-assemble into aggregates thus increasing the thickness of the interface. Yet, the initially measured surface

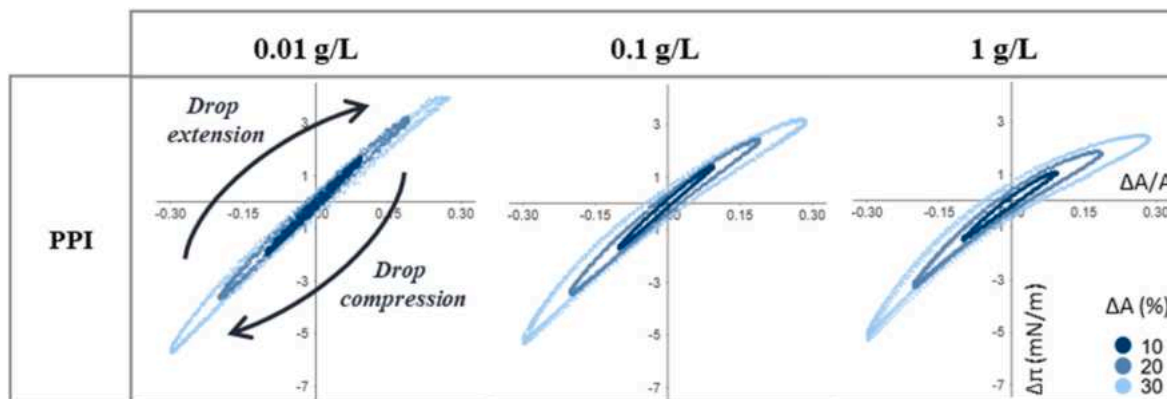


Fig. 4. Lissajous plots showing the variation in surface pressure ($\Delta\pi$, mN/m) against the applied deformation ($\Delta A/A$) of interfacial films prepared with the soluble fractions of PPI. Three different protein concentrations were tested: 0.01 g/L (column 1), 0.1 g/L (column 2), and 1 g/L (column 3). Three different dilatational deformations (10 %, 20 %, or 30 % variation of the drop area, from darker to lighter shade) are represented and were measured at a constant frequency of 0.02 Hz. The pending drop had an initial surface area of 30 mm². Y-axis, representing surface pressure change, goes from -7 to $+4$ mN/m. Experiments were performed in independent triplicates, and representative curves are provided here.

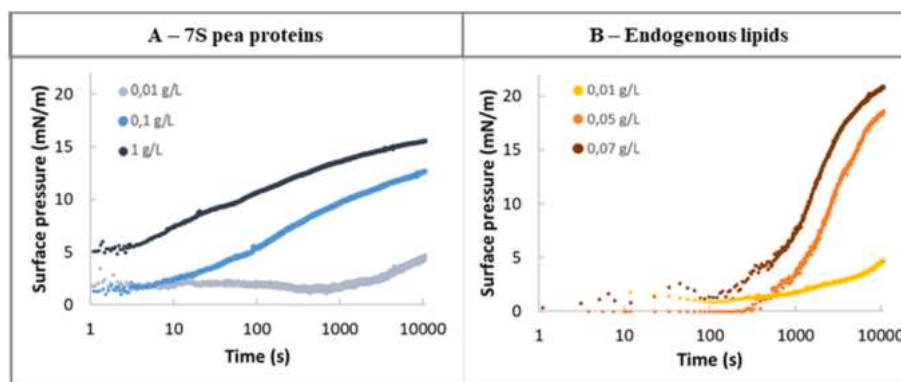


Fig. 5. Adsorption kinetics of 7S pea proteins (A) or endogenous lipid dispersions (B), showing the surface pressure (mN/m) as a function of time (s). Three concentrations were probed, 0.01 g/L, 0.1 g/L and 1 g proteins/L for 7S proteins, and 0.01 g/L, 0.05 g/L and 0.07 g lipids/L for the lipid dispersion.

pressure at 1 g/L is slightly lower for 7S proteins (about 8 mN/m) compared to PPI (about 11 mN/m). This difference is likely assignable to experimental error, though the role of other components present in the soluble fraction of isolates cannot be disregarded (other proteins than vicilins/convicilins, peptides, endogenous phospholipids, other non-proteinaceous compounds, potential complexes of proteins with endogenous phenolics, etc.).

Adsorption kinetics for the lipid dispersions are given in Fig. 5B. For the lowest lipid concentration tested (0.01 g/L), very low surface pressures were reached even after 3 h (around 5 mN/m). The increase in surface pressure began after around 1000 s, similarly to what was observed for the highest concentration (0.07 g/L), which shows that

adsorption proceeded slowly. Yet, for 0.05 and 0.07 g/L, the surface pressure increased substantially, reaching around 18–20 mN/m after 3 h. We presume that in such an aqueous dispersion, lipids (of which 64 wt % of polar lipids and 36 wt% of triglycerides, section 3.1) organize themselves into spherical vesicles (liposomes), very small droplets, micelles or unilamellar to multilamellar assemblies (Chen & Sagis, 2019). Those structures therefore diffuse slowly towards the interface, bound to the latter and disintegrate thus allowing single phospholipids to reach the interface into phospholipid monolayers (Chen & Sagis, 2019; Wanninge et al., 2005). The increase in surface pressure is therefore observed once enough surface-active material is covering the interface (contact points) (Yang et al., 2023). Comparing these results with

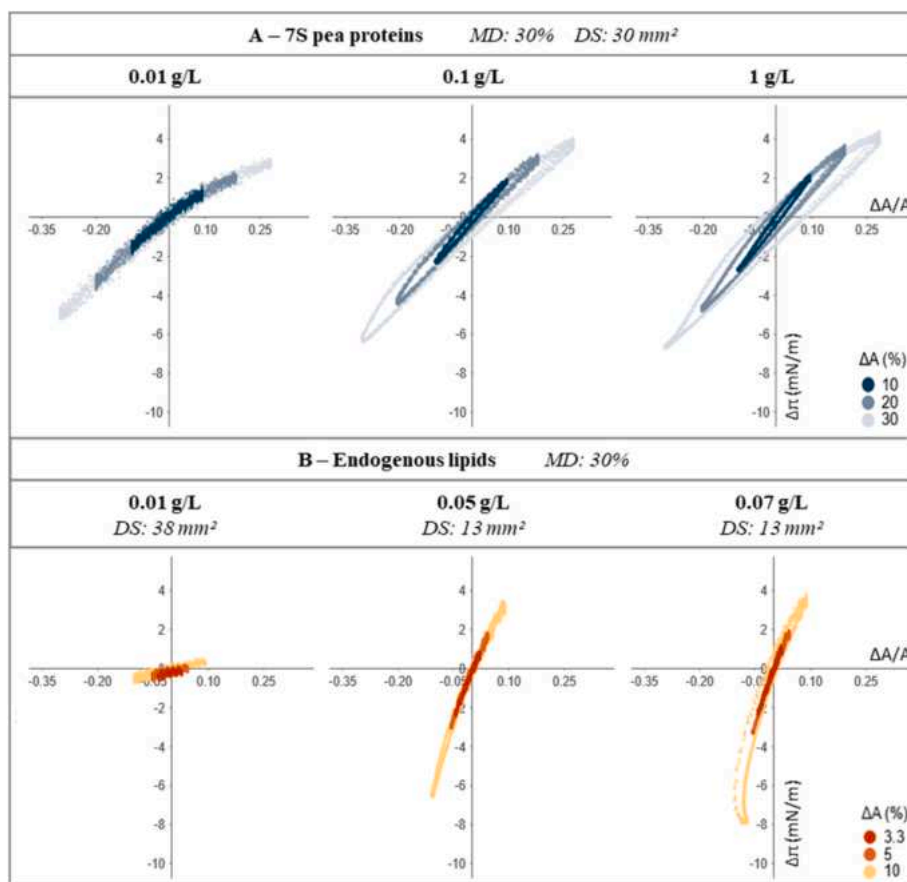


Fig. 6. Lissajous plots for interfaces formed by (A) purified 7S pea proteins at 0.01; 0.1 or 1 g/L at three dilatational deformations (10 %, 20 %, 30 %) of a pending drop of 30 mm². (B) Lissajous plots of interfaces formed by an endogenous lipid dispersion at 0.01; 0.05 or 0.07 g/L at three dilatational deformations (3.3 %, 5 %, 10 %) of a pending drop of 38 or 13 mm². MD: maximum deformation. DS: drop surface area.

available data in the literature can be challenging, as polar lipids are often dispersed in an apolar phase (chloroform or oil) (Bernaschina et al., 2024; Deleu et al., 2010; He et al., 2008).

3.2.2. Behaviour of the interfacial films under oscillatory dilatational deformation

The rheological properties of interfacial films based on 7S pea proteins are shown in Fig. 6A. An elastic interfacial film was generated at 0.01 g/L, showing slight strain softening in extension. When increasing protein concentration, the viscous contribution increased moderately, leading to viscoelastic interfacial films. This behaviour is typical for globular proteins (Cai et al., 2023), and was also demonstrated to occur at the air-water interface (Shen, Luo, & et al, 2023). No strong asymmetric behaviours occur at the maximum extension and compression, suggesting that the interfacial film is not strongly affected by the applied deformation. Some authors studied vicilins from red kidney beans, and showed that structural rearrangements of the adsorbed proteins ruled over the capacity of the proteins to diffuse and penetrate at the interface: it seems that the flexibility of the proteins is key in enhancing their interfacial rearrangements at the oil-water interface (Liang & Tang, 2013). Moreover, vicilins appear to have significantly higher rearrangement capacities compared to their counterparts legumins or albumins at the air-water interface (Shen, Luo, & et al, 2023).

The rheological features of the interfacial films formed from the lipid dispersions were also assessed (Fig. 6B). For the lowest concentration, the slope of the Lissajous plot is very low: there is no significant surface pressure change upon the deformations (until 10 % of change of the drop surface area). Next to the very low surface pressure measured at this concentration (Fig. 5B), this behaviour suggests that the lipids are in an expanded phase. Conversely, for 0.05 and 0.07 g/L, the plots showed very extensive variations of the surface pressure (almost 12 mN/m in absolute value), even for moderate deformations. This rheological behaviour indicates that the interface strongly resists deformation and thus has a behaviour which resembles that of a solid film (Ikenaga & Sagis, 2024; Yang et al., 2023).

The rheological signatures of pea proteins and pea lipids are thus dramatically different, which led us to wonder how mixes thereof would behave, in particular with the protein-to-lipid mass ratio naturally occurring in PPI, i.e., 6:1.

3.3. Behaviour of mixes of the purified components at the oil-water interface

3.3.1. Adsorption kinetics

Model systems made of solutions of purified 7S pea proteins in which extracted pea lipids were dispersed were prepared at three different protein-to-lipid mass ratios (1:6, where lipids are prominent, 1:1, where proteins and lipids are present in equal amounts; and 6:1, mimicking the ratio inherently found in PPI). As observed previously, the dispersion of endogenous lipids showed strong surface activity even for a concentration as low as 0.07 g/L. This concentration was therefore chosen as the maximum one for the three model systems; besides, preliminary trials showed that too high concentrations led to detaching the drop from the needle during the experiment.

In Fig. 7, for each ratio, the adsorption kinetics for the purified proteins or lipids with matching concentrations are superimposed over the kinetic of the mix to facilitate comparison with the individual components. For the 1:6 ratio, the adsorption behaviour of the mix mostly followed the trend observed for pure lipids. As major components, the latter dictate the surface-active properties over proteins. Yet, at the onset of the experiment, surface pressure seemed somewhat higher for the mix than for the pure components. Although this corresponds to the part of the experiment where the recorded signal was noisy, this might result from a synergetic effect between phospholipids and proteins. When the ratio was 1:1, we observed the same phenomenon, where the adsorption kinetics of the mix ended with the same signature as the kinetics with pure lipids; this suggests that in a sample where proteins and lipids would be present in equal mass amounts, phospholipids would dominate the interface within relatively short time periods (3 h). For the 6:1 ratio, the adsorption kinetics were less easily ascribable to one of the individual constituents; interestingly, the eventual surface pressure reached with the mix was lower than those attained with either pure proteins or pure lipids. Nevertheless, the initial values of surface pressures were around 5 mN/m both for pure proteins and for the 6:1 mix, suggesting that proteins prevail at the interface over lipids, at least at very short times. Some authors also observed that a mix of phospholipids (dioleoylphosphatidylcholine, DOPC) with proteins (β -casein) did not show similar or purely additive properties compared to the individual components. They explained this by the potential existence of specific interactions, where less hydrophilic and less surface-active complexes would be formed (Fang & Dalgleish, 1996).

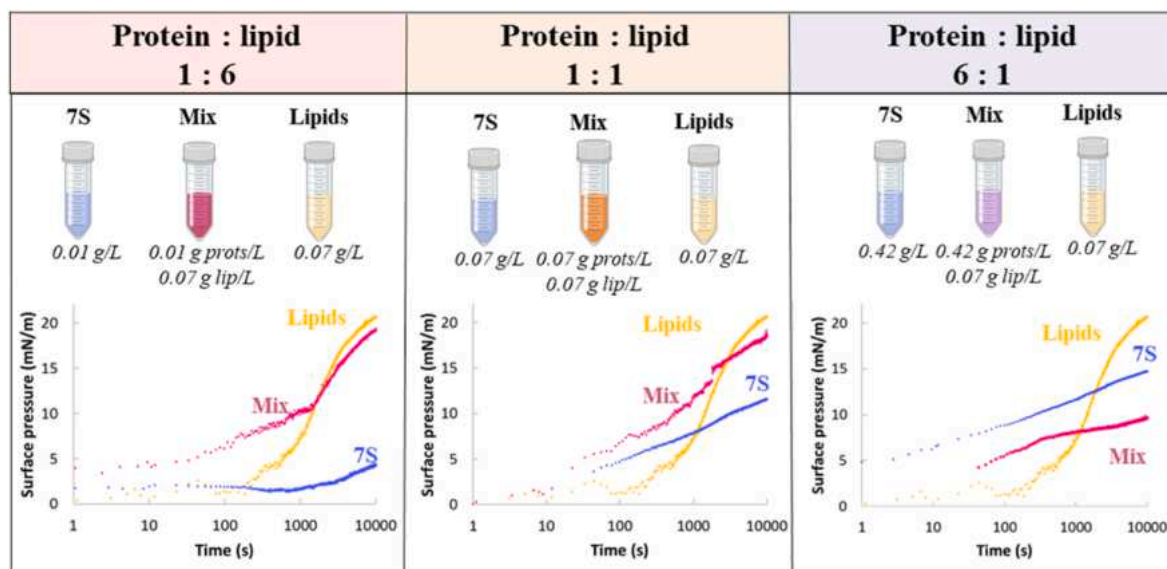


Fig. 7. Adsorption kinetics of the systems made of purified 7S pea proteins (blue curve), purified pea lipids (yellow curve), and their mixes (pink curve) for three protein-to-lipid ratios (w/v) (1:6; 1:1 and 6:1). The concentrations probed for each of the three systems are recalled on top of the graphs.

3.3.2. Behaviour of the interfacial films under oscillatory dilatational deformation

Lissajous curves of the mixes were then studied, from pure proteins to pure lipids (Fig. 8, from left to right). As observed with the 6:1 ratio, a slight addition of lipids (0.07 g/L) to a protein solution (0.42 g/L) induced a clear strain softening behaviour in extension when compared to sole proteins at the same concentration. Strain-hardening behaviour in compression was also visible. This rheological signature indicates that for this ratio, which is the same as inherently found in the soluble fraction of PPI, the interfacial film comprises not only proteins but also phospholipids, which probably compete for adsorption. Accordingly, the interfacial behaviour generated with this model system (ratio 6:1) looked very similar to that observed for the soluble fraction of PPI (Fig. 4). It should be noted that proteins in PPI encompass many other categories than 7S proteins (e.g., 11S legumins, 2S albumins), with potentially different colloidal organization and interfacial properties (Shen, Li, & et al, 2023). The colloidal organization of endogenous lipids in PPI is also far from unravelled, which certainly influences their interfacial properties.

When moving to ratios of 1:1, and then 1:6, we observed an increasing strength of the interfacial film (i.e., high $\Delta\pi$ values) and strain hardening behaviour in compression, with a strong increase in the magnitude of the slopes of the tangent to the curve. This characterizes stiff, solid-like interfaces that strongly resist deformation, as previously observed for the system with pure lipids (Fig. 6B). In addition, when high proportions of lipids were used, the drop surface area could not exceed 13 mm² (against 30 mm²), and the deformation extent that could be applied was also limited. When exceeding these conditions, the drop detached from the needle because of the very high surface pressures reached (up to 25–26 mN/m; data not shown). At these ratios, we may assume that proteins would be displaced from the interface by the highly surface-active polar lipids.

The interfacial and emulsifying properties of mixes of PPI with phospholipids were investigated in another recent study. In particular, displacement of proteins by phospholipids was highlighted using proteomics, and 7S pea proteins were preferentially displaced compared to 11S legumins (Shen, Zheng, & et al, 2023). Those results are consistent with the present ones, although the mechanisms for adsorption are different: mass transfer at high shear rates (homogenization) in the first case, vs spontaneous diffusion in the present study. Recently, an equivalent methodological approach was carried out on mixtures of

when protein isolate with escin (a water-soluble LMWE from the family of saponins, for instance extracted from horse chestnut). It revealed that at mass ratios of 1:1 and 1:3 (WPI:escin), escin dictated the rheological behaviour of the mixed films at the air-water interface (Yang et al., 2023).

3.4. Structural organization of the films formed at the air-water interface

3.4.1. Adsorption and ellipsometric angle kinetics

To further characterize the organization of the PPI-based interfacial films, more work was carried out at the air-water interface using a Langmuir trough. The objective was to investigate the interfacial behaviour of the films made of purified proteins (0.1 g/L), extracted lipids only (0.07 g/L), and of PPI at two extreme concentrations (0.01 g/L and 1 g/L) to highlight the different competitive processes for adsorption between proteins and phospholipids. To remain close to the experimental design used in the drop tensiometry experiments, the aqueous solutions/dispersions were directly poured as the subphase in a Langmuir trough, and the adsorption kinetics of the amphiphilic molecules at the air-water interface were monitored for 3 h. During this time, surface pressure, reflecting the lateral interactions between the amphiphilic molecules, and ellipsometric angle, reflecting the film thickness, were recorded simultaneously (Fig. 9).

PPI at the highest concentration (1 g/L) led to a very different evolution of π and Δ over time compared to the diluted PPI suspension (0.01 g/L). Indeed, the kinetics showed an increase of surface pressure and ellipsometric angle right after the suspension was poured in the Langmuir trough, indicating a fast adsorption of amphiphilic molecules. Oppositely, for diluted PPI, π only started to increase after 200 s, displaying different stages of protein interfacial arrangements, as previously described (Fig. 3). Concerning the dispersion of pea lipids (0.07 g/L), even faster adsorption kinetics were observed compared to PPI (1 g/L), with values of π and Δ achieving a plateau almost instantaneously after the suspension was poured in the Langmuir trough. This indicated a very rapid diffusion and adsorption of surface-active lipids at the air-water interface. This behaviour contrasts with the one at the oil-water interface (Fig. 3) of the same sample, where the increase in surface pressure was much longer compared to the present air-water adsorption kinetic.

After 3 h, π and Δ reached values close to 21.5 mN/m for both and 13° or 14.2°, respectively, for PPI (0.01 g/L) and 7S pea protein (0.1 g/L)

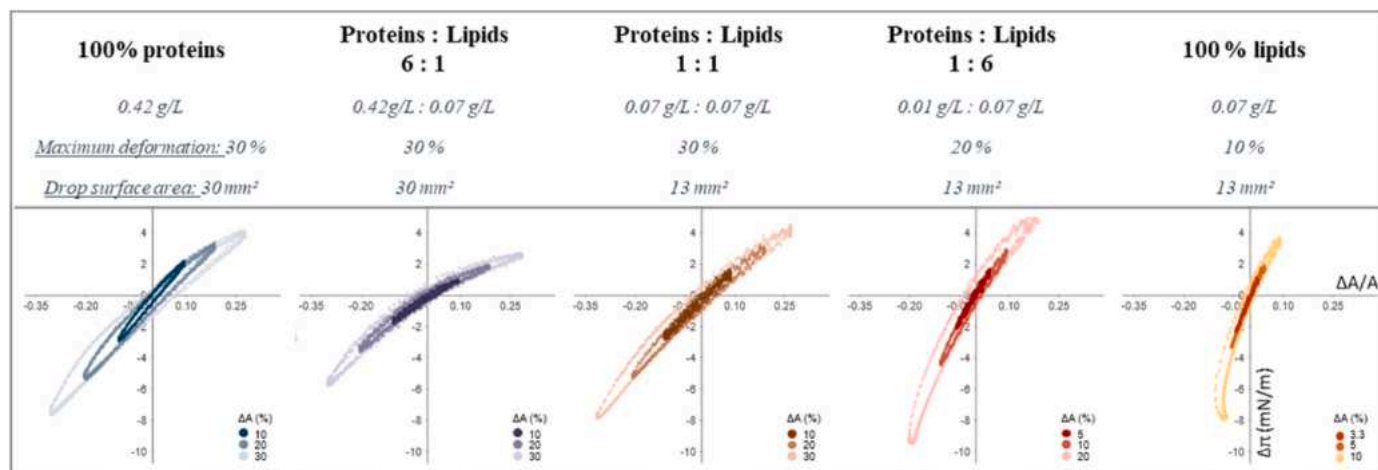


Fig. 8. Lissajous plots showing the variation in surface pressure ($\Delta\pi$, mN/m) against deformation ($\Delta A/A$) from interfacial films prepared with different protein-to-lipid ratios: from pure protein (7S) solutions (0.42 g/L), to pure lipid dispersion (0.07 g/L). The data obtained for protein-to-lipid mass ratios of 6:1; 1:1 and 1:6 are presented in between, with respective concentrations given above the plots. Three different dilatational deformations are given for each plot (from darker to lighter shade) which are specified on each plot. Amplitude sweeps were performed at a constant frequency of 0.02 Hz, at a drop surface area of 30 mm² or 13 mm², as indicated above the plots. Y-axes, representing surface pressure change, range from −10 to +5 mN/m. Experiments were performed in independent duplicates or triplicates, and representative curves are provided here.

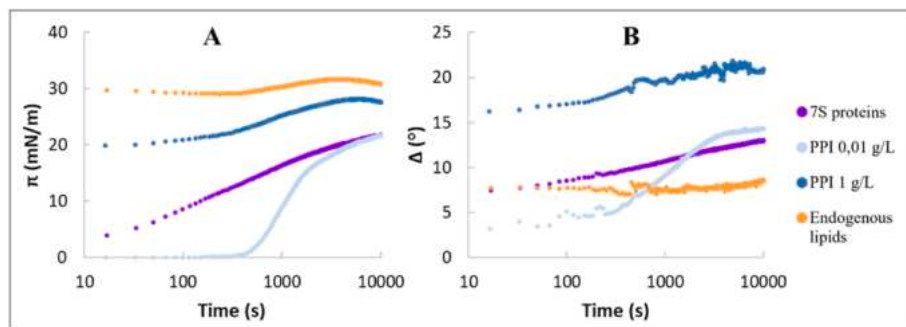


Fig. 9. (A) Surface pressure (mN/m) as a function of log (time (s)) after infusing aqueous solutions/dispersions of different components in the subphase of a Langmuir trough filled with buffer: 7S pea proteins (0.1 g/L), the soluble fraction of PPI at two concentrations (0.01 or 1 g/L) or a dispersion of extracted lipids from PPI (0.07 g/L). (B) Corresponding ellipsometric angle (°) as a function of log (time). Representative curves are provided for (A) and (B) out of independent replicates.

suspensions. It indicates that both films may share an organization led by similar lateral interactions, in agreement with the results obtained at the oil-water interface. For PPI (1 g/L), the surface pressure and ellipsometric angle reached a plateau after 1200 s, and final values of 25 mN/m and 20° were obtained. Such results are consistent with the interfacial microstructure, rich in protein aggregates, as described in the next section (section 3.4.2). Yet, the ellipsometric measurement for this sample was quite noisy, which could be due to structural heterogeneity of the film at length scales relevant to the resolution of the measurement. For the lipid dispersion, final values of 30 mN/m and 8° were obtained after 3 h for π and Δ respectively, which are close to previously reported ones for a natural blend of saturated and unsaturated phospholipids (Bourlieu et al., 2020).

Some differences can be highlighted regarding the kinetics of PPI (0.1 g/L) and 7S proteins. They lied in a slower increase of the surface pressure and ellipsometric angle for PPI compared to the purified 7S suspension, reflecting a slower adsorption. This slower diffusion of the amphiphilic molecules toward the air-water interface may be partially explained by a different conformation of the 7S proteins, as well as by a competition phenomenon between the various surface-active molecules in the PPI suspension. The higher final values of π and Δ with the concentrated PPI suspension (1 g/L) compared to the diluted one (0.01 g/L), as well as the differences observed in the adsorption kinetics, reveal the formation of a thicker film in the former case. Nonetheless, all the samples (except the lipid dispersion) share important similarities between the air-water adsorption kinetics with the oil-water adsorption kinetics obtained by drop tensiometry (Figs. 3 and 7).

Several researches used ellipsometry measurements to quantitatively analyze the thickness of interfacial films stabilized by plant proteins. For instance, air-water interfacial films stabilized by pea or rapeseed proteins were around 2–6 nm thick (Hinderink et al., 2020; Yang et al., 2021). Further studies showed that heat-treated and/or spray-dried pea proteins would result in the formation of thin interfacial films, likely to be constituted by albumins, since highly aggregated proteins (aggregates larger than 200 nm) are unlikely to be surface-active (Yang et al., 2022). It is worth reminding that here, the soluble fraction of PPI had been treated by HPH, which generated smaller protein aggregates than in the initial suspension (about 58 nm (Keuleyan et al., 2023)). Recently, some authors measured the thickness of Langmuir-Blodgett films generated with a commercial PPI treated by HPH deposited with a syringe on the subphase. They found heights of 3.4 nm. Yet smaller than the size of the aggregates measured by dynamic light scattering, they suggested that small surface-active particles would be more prone to adsorb at the interface compared to bigger particles (Grasberger et al., 2024).

Overall, the present results are in line with the outcomes obtained by drop tensiometry at the oil-water interface, highlighting contrasted diffusion processes and interfacial organizations depending on the concentration of the suspension.

3.4.2. Microstructure of the air-water interfacial Langmuir-Blodgett films

To get further insights into the structural organization of the interfacial films, Langmuir-Blodgett transfer were performed at the end of each experiment (3-h kinetics). The films were transferred on mica sheets and then observed by atomic force microscopy (AFM, as previously performed (Kergomard et al., 2022)), yielding topography images and corresponding height profiles (Fig. 10).

The film of purified pea proteins 7S appeared to be quite homogeneous (average height against the background of 3.4 ± 0.4 nm on profile a and 3.4 ± 0.5 nm on profile b), with some aggregates distributed all over the sample (maximal height of 13.6 μ m, profile a). The film of the lipid dispersion appeared more heterogeneous, with the presence of three main kinds of domains in addition to the fluid background, which was likely composed by unsaturated lipids. Circular domains of less than 0.5 nm height were visible, probably mainly composed by organized saturated lipids, on which high clusters of 4.8 ± 1.2 nm (profile d) to 7.6 nm in height can be observed (illustrated by arrow 2, profile c). A possible explanation would be that the high clusters act as nuclei around which the circular domains expand and eventually merge together. Another explanation to the presence of such structures could be the presence of residual endogenous proteins in the lipid extract. For instance, highly hydrophobic oleosins might be extracted with the chloroform/methanol solvent, and according to the literature, such peaks could correspond to oleosins (Kergomard et al., 2021; Zielbauer et al., 2018). In a study by (Kergomard et al., 2021) on the interfacial behaviour of oleosomes from walnuts, similar structures were attributed to triacylglycerol-, phospholipid- and oleosin assemblies. Apart from these circular domains, flower-shaped structures of 1.4 and 1.7 nm in height were also observed (profile c and d, respectively). Such irregular domain boundaries could result from a low line tension between the unsaturated lipids composing the background and the ones composing the organized domains, thus indicating partial miscibility (Kergomard et al., 2022). Some authors showed that they could result from the coexistence of both condensed and expanded liquid phases among phospholipid monolayers (Möhwald, 1990; Rodríguez Patino et al., 2007; Vié et al., 1998).

Based on the images obtained from both purified protein and lipid films, the very heterogeneous and complex interfacial microstructures from the two PPI films could be interpreted. The images from the lowest concentration (0.01 g/L) showed the presence of large clusters from 6 to 13 nm in height (profiles e and f), which could correspond to protein aggregates. Very small domains (black arrows) were also visible, and might correspond to lipid-based domains, that are present on the film, yet without affecting their rheological properties (strongly elastic Lissajous plots for PPI 0.01 g/L, Fig. 4). Moving on to the film formed with concentrated PPI (1 g/L), the height of the clusters was much higher (until 37 nm, as illustrated on height profile g), and the smaller domains were much larger and even more noticeable than for the diluted sample, forming “holes” (in-between arrows 6 and 7 on profile g; and 8 and 9 on

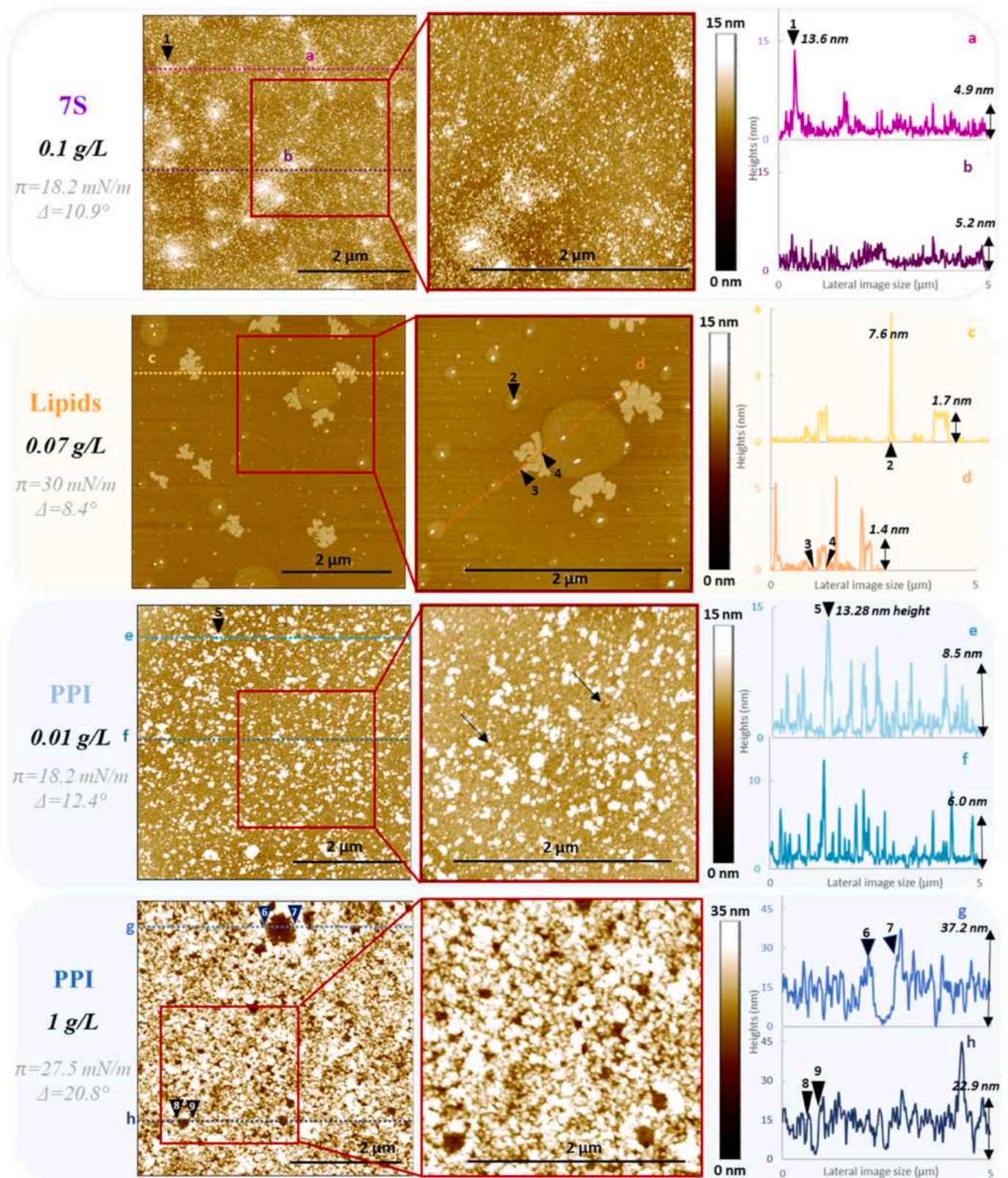


Fig. 10. Atomic force microscopy (AFM) images (left: $5 \mu\text{m} \times 5 \mu\text{m}$, scale bar $2 \mu\text{m}$; right: $2.5 \mu\text{m} \times 2.5 \mu\text{m}$, scale bar $2 \mu\text{m}$) of the Langmuir-Blodgett films made from the 7S pea protein solution (0.1 g/L), PPI soluble fraction at 0.01 and 1 g/L, and from the dispersion of endogenous lipids (0.07 g/L). The surface pressures and ellipsometric angles indicate the conditions during film sampling on the mica substrate (left column). The coloured lines on the AFM images indicate where the heights profiles were measured. Red arrows on the image of PPI (0.01 g/L) indicate smaller domains amongst the clusters. Arrows on the AFM images for PPI (1 g/L) and lipids represent the corresponding peaks of the height profiles.

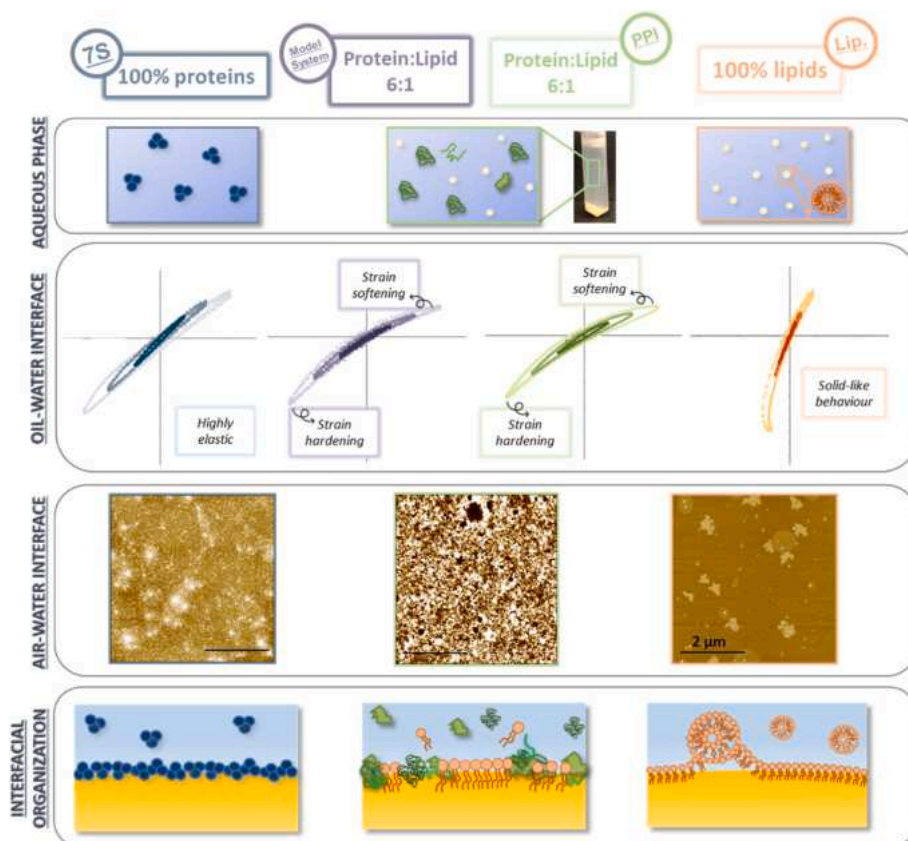


Fig. 11. Graphical sum up of the results obtained in this study. Several samples were used as aqueous phases, with different protein and lipid composition, stemming from pea (row 1). Their interfacial rheological behaviour was screened at the oil-water interface by drop tensiometry, providing representations with Lissajous plots (row 2). The experimental set up was closely reproduced in a Langmuir trough, in order to get more insights into the air-water interfacial properties of the films, that were observed by AFM (row 3). All these results lead to consider the formation of mixed oil-water interfacial films stemming from the competition between proteins and lipids, as illustrated in row 4.

profile g) with respect to the average aggregate background. These lower structures are very likely to correspond to lipid domains, distributed over the interfacial film. HPH treatment being the cause for releasing lipid-containing structures (Keuleyan et al., 2023), the present film for PPI was complementary to existing characterization of air-water interfaces (not treated by HPH, where only protein clusters are visible (Hinderink, 2021)). We therefore demonstrate that both proteins and polar lipids from a protein ingredient may adsorb and co-exist at fluid interfaces.

Complex and composite interfacial films were generated, which may be associated to their peculiar rheological signature, as illustrated and summarized in Fig. 11. These results can help understanding the mechanisms involved in the stabilization of emulsified oil droplets when complex ingredients containing multiple surface-active molecules are used. In particular, identifying the nature of the interfacial compounds adsorbed at the interface and analyzing the mechanical properties of the interfacial films can help predicting potential droplet-droplet interactions. This, in turn, enables better control over the emulsification process in dispersed food systems and the management of their destabilization mechanisms. One limitation of the present approach lies in the diffusion mechanisms of surface-active molecules toward the interface and the low aqueous phases concentrations required. Conversely, high shear occurs during conventional homogenization processes, which drives interfacial adsorption and competition. Future work will therefore be instrumental to evaluate the competition between proteins and endogenous lipids from PPI at the scale of an emulsified system.

4. Conclusions

In this study, we showed that the soluble fraction of a PPI aqueous suspension contains proteins and phospholipids, which compete for adsorption at oil-water and air-water interfaces. We combined complementary approaches to decipher the respective contributions of the individual components and compared them to the overall interfacial mechanical properties of interfacial films stabilized by the commercial PPI. The formation of mixed interfacial films according to the protein-to-lipid ratio was demonstrated. Based on dilatational oscillatory deformations and Lissajous curves, we showed that at low bulk concentrations, adsorbed lipids have a minimal contribution to the rheological behaviour of PPI-based films. Conversely, at higher bulk concentration, lipids form distinct domains at the interface and substantially affect the rheological dilatational properties of the interface, resulting in a lower connectivity and mechanical strength of the interfacial film during extension. It should be noted that potential interferences in drop tensiometry may arise from the shear elasticity of the interfacial proteinaceous network, which would require to add fitting elastometry to the classic drop tensiometry methodology.

This work challenges existing literature by proving that despite these ingredients are named “protein ingredients” (and used primarily as a source of proteins for nutritional and technological incentives), these constituents are not solely responsible for their interfacial properties. The existence of endogenous polar lipids at the interface reshuffles the cards of our understanding of the stabilization mechanisms of food products using those ingredients, for which non-proteinaceous compounds cannot be disregarded. Questions remain on whether such competitive processes are also at stake in emulsification conditions, as

another key parameter for this competition is the available surface area. Hence, studying the time evolution of such interfaces is also necessary, since the competition between proteins and phospholipids is a long-time process, and protein displacement is likely to occur over long timescales.

Fine-tuning the functionality of emulsified food products begins with the understanding of the interface, its composition, and its mechanical properties. The present outcomes highlight that with a rational use of food processing combined with a deep compositional and functional characterization, the natural complexity of plant protein ingredients can be an asset for future food formulations.

CRediT authorship contribution statement

Eléna Keuleyan: Writing – review & editing, Writing – original draft, Visualization, Validation, Methodology, Investigation, Formal analysis, Data curation, Conceptualization. **Jeanne Kergomard:** Writing – review & editing, Visualization, Validation, Methodology, Investigation, Formal analysis, Data curation, Conceptualization. **Ade-line Boire:** Writing – review & editing, Software, Data curation. **Elisabeth David-Briand:** Writing – review & editing, Methodology, Investigation, Formal analysis. **Véronique Vié:** Writing – review & editing, Visualization, Validation. **Anne Meynier:** Writing – review & editing, Visualization, Validation, Supervision, Funding acquisition. **Alain Riaublanc:** Writing – review & editing, Visualization, Validation, Supervision, Project administration, Methodology, Funding acquisition, Conceptualization. **Claire Berton-Carabin:** Writing – review & editing, Visualization, Validation, Supervision, Project administration, Methodology, Funding acquisition, Conceptualization.

Declaration of competing interest

The authors declare that they have no known competing financial interests or personal relationships that could have appeared to influence the work reported in this paper.

Acknowledgements

The authors would like to thank the **2CBioMIF platform** (IPR-ScanMAT Rennes, France) for the interfacial characterization of the samples at the air-water interface (ellipsometry, tensiometry, AFM). **Alice Kermarrec** is thanked for her advices with the optimization of lipid extraction. **Véronique Solé-Jamault** and **Joëlle Davy** are thanked for the purification of 7S proteins. The financial support of EK's PhD grant, and of CBC's Connect Talent "VESTA" grant by Région Pays de la Loire and Nantes Métropole is gratefully acknowledged.

Appendix A. Supplementary data

Supplementary data to this article can be found online at <https://doi.org/10.1016/j.foodhyd.2025.111475>.

Data availability

Data will be made available on request.

References

- Amagliani, L., & Schmitt, C. (2017). Globular plant protein aggregates for stabilization of food foams and emulsions. *Trends in Food Science and Technology*, 67, 248–259. <https://doi.org/10.1016/j.tifs.2017.07.013>
- Azzam, R. M. A., Bashara, N. M., & Balard, S. S. (1978). Ellipsometry and polarized light. *Physics Today*, 31(11), 72.
- Berge, B., & Renault, A. (1993). Ellipsometry study of 2d crystallization of 1-alcohol monolayers at the water surface. *EPL*, 21(7), 773–777. <https://doi.org/10.1209/0295-5075/21/7/010>
- Bergfreund, J., et al. (2021). Surfactant adsorption to different fluid interfaces. *Langmuir*, 37(22), 6722–6727. <https://doi.org/10.1021/acs.langmuir.1c00668>

- Bernaschina, M., et al. (2024). Lentil protein stabilized emulsion - impact of lecithin addition on emulsions properties. *Food Hydrocolloids*, 147(PA), Article 109337. <https://doi.org/10.1016/j.foodhyd.2023.109337>
- Berton-Carabin, C., et al. (2013). Design of interfacial films to control lipid oxidation in oil-in-water emulsions. *Food Hydrocolloids*, 33(1), 99–105. <https://doi.org/10.1016/j.foodhyd.2013.02.021>
- Berton-Carabin, C., Ribourg-Birault, L., & Benatti Gallo, T. C. (2024). Stripping of vegetable oils by direct mixing with adsorbent materials. In C. Lopez, C. Genot, & A. Riaublanc (Eds.), *Multidimensional Characterization of dietary lipids. Humana*. New-York: Springer US.
- Berton-Carabin, C., Sagis, L., & Schroeën, K. (2018). Formation, structure, and functionality of interfacial layers in food emulsions. *Annual Review of Food Science and Technology*, 9, 551–587. <https://doi.org/10.1146/annurev-food-030117>
- Beverung, C. J., Radke, C. J., & Blanch, H. W. (1999). Protein adsorption at the oil/water interface: Characterization of adsorption kinetics by dynamic interfacial tension measurements. *Biophysical Chemistry*, 81(1), 59–80. [https://doi.org/10.1016/S0301-4622\(99\)00082-4](https://doi.org/10.1016/S0301-4622(99)00082-4)
- Bligh, E. G., & Dyer, W. J. (1959). A rapid method of total lipid extraction and purification. *Canadian Journal of Biochemistry and Physiology*, 37(8), 911–917.
- Bos, A. M., & van Vliet, T. (2001). Interfacial rheological properties of adsorbed protein layers and surfactants: A review. *Advances in Colloid and Interface Science*, 91, 437–471.
- Botti, T. C., et al. (2022). Effect of interfacial rheology on drop coalescence in water-oil emulsion. *Soft Matter*, 18(7), 1423–1434. <https://doi.org/10.1039/d1sm01382c>
- Bourlieu, C., et al. (2020). Physico-chemical behaviors of human and bovine milk membrane extracts and their influence on gastric lipase adsorption. *Biochimie*, 169, 95–105. <https://doi.org/10.1016/j.biochi.2019.12.003>
- Burger, T. G., et al. (2021). Comparison of physicochemical and emulsifying properties of commercial pea protein powders. *Journal of the Science of Food and Agriculture*, (October) <https://doi.org/10.1002/jsfa.11592>
- Cai, Z., et al. (2023). Correlation between interfacial layer properties and physical stability of food emulsions: Current trends, challenges, strategies, and further perspectives. *Advances in Colloid and Interface Science*, 313(February), Article 102863. <https://doi.org/10.1016/j.cis.2023.102863>
- Caro, A. L., Niño, M. R. R., & Patino, J. M. R. (2009). The effect of pH on structural, topographical, and rheological characteristics of β -casein-DPPC mixed monolayers spread at the air-water interface. *Colloids and Surfaces A: Physicochemical and Engineering Aspects*, 332(2–3), 180–191. <https://doi.org/10.1016/j.colsurfa.2008.09.020>
- Chang, C., et al. (2015). Effect of pH on the inter-relationships between the physicochemical, interfacial and emulsifying properties for pea, soy, lentil and canola protein isolates. *Food Research International*, 77, 360–367. <https://doi.org/10.1016/j.foodres.2015.08.012>
- Chen, J. S., Dickinson, E., & Iveson, G. (1993). Interfacial interactions, competitive adsorption and emulsion stability. *Food Structure*, 12(2), 135–146.
- Chen, & Sagis, L. (2019). The influence of protein/phospholipid ratio on the physicochemical and interfacial properties of biomimetic milk fat globules. *Food Hydrocolloids*, 97(April), Article 105179. <https://doi.org/10.1016/j.foodhyd.2019.105179>
- Clark, D. C., et al. (1994). Differences in the structure and dynamics of the adsorbed layers in protein-stabilized model foams and emulsions. *Faraday Discussions*, 98, 253–262. <https://doi.org/10.1039/FD9949800253>
- Coke, M., et al. (1990). The influence of surface composition and molecular diffusion on the stability of foams formed from protein/surfactant mixtures. *Journal of Colloid and Interface Science*, 138(2), 489–504. [https://doi.org/10.1016/0021-9797\(90\)90231-C](https://doi.org/10.1016/0021-9797(90)90231-C)
- Courthaudon, J. L., Dickinson, E., & Dalgleish, D. G. (1991). Competitive adsorption of β -casein and nonionic surfactants in oil-in-water emulsions. *Journal of Colloid and Interface Science*, 145(2), 390–395. [https://doi.org/10.1016/0021-9797\(91\)90369-J](https://doi.org/10.1016/0021-9797(91)90369-J)
- Dagorn-Scaviner, C., Gueguen, J., & Lefebvre, J. (1987). Emulsifying properties of pea globulins as related to their adsorption behaviors. *Journal of Food Science*, 52(2), 335–341. <https://doi.org/10.1111/j.1365-2621.1987.tb06607.x>
- Deleu, M., et al. (2010). Interfacial properties of oleosins and phospholipids from rapeseed for the stability of oil bodies in aqueous medium. *Colloids and Surfaces B: Biointerfaces*, 80(2), 125–132. <https://doi.org/10.1016/j.colsurfb.2010.05.036>
- Dickinson, E., Murray, B. S., & Stainsby, G. (1988). Coalescence stability of emulsion-sized droplets at a planar oil-water interface and the relationship to protein film surface rheology. *Journal of the Chemical Society, Faraday Transactions 1: Physical Chemistry in Condensed Phases*, 84(3), 871–883. <https://doi.org/10.1039/F19888400871>
- Drusch, S., Klost, M., & Kieserling, H. (2021). Current knowledge on the interfacial behaviour limits our understanding of plant protein functionality in emulsions. *Current Opinion in Colloid & Interface Science*, 56, Article 101503. <https://doi.org/10.1016/j.cocis.2021.101503>
- Fang, Y., & Dalgleish, D. G. (1996). Competitive adsorption between dioleoylphosphatidylcholine and sodium caseinate on oil-water interfaces. *Journal of Agricultural and Food Chemistry*, 44(1), 59–64. <https://doi.org/10.1021/jf950330g>
- Folch, J., Lees, M., & Sloane Stanley, G. H. (1957). A simple method for the isolation and purification of total lipides from animal tissues. *Isolation of Total Tissue Lipides*, 497–509.
- Graham, D. E., & Phillips, M. C. (1980). Proteins at liquid interfaces. IV. Dilatational properties. *Journal of Colloid and Interface Science*, 76(1), 227–239. [https://doi.org/10.1016/0021-9797\(80\)90289-1](https://doi.org/10.1016/0021-9797(80)90289-1)
- Grasberger, K., et al. (2022). Behavior of mixed pea-whey protein at interfaces and in bulk oil-in-water emulsions. *Innovative Food Science & Emerging Technologies*, 81. <https://doi.org/10.1016/j.ifset.2022.103136>

- Grasberger, K., et al. (2024). Role of the pea protein aggregation state on their interfacial properties. *Journal of Colloid and Interface Science*, 658(July 2023), 156–166. <https://doi.org/10.1016/j.jcis.2023.12.068>
- Grasberger, K., Hammershøj, M., & Corredig, M. (2023). Stability and viscoelastic properties of mixed lupin-whey protein at oil-water interfaces depend on mixing sequence. *Food Hydrocolloids*, 138(January). <https://doi.org/10.1016/j.foodhyd.2023.108485>
- He, Q., et al. (2008). Dynamic adsorption and characterization of phospholipid and mixed phospholipid/protein layers at liquid/liquid interfaces. *Advances in Colloid and Interface Science*, 140(2), 67–76. <https://doi.org/10.1016/j.cis.2007.12.004>
- Hinderink, E. B. A. (2021). *Food emulsions stabilised by blends of plant and dairy proteins*. Wageningen University & Research.
- Hinderink, E. B. A., et al. (2020). Behavior of plant-dairy protein blends at air-water and oil-water interfaces. *Colloids and Surfaces B: Biointerfaces*, 192(April), Article 111015. <https://doi.org/10.1016/j.colsurfb.2020.111015>
- Ikenaga, N., & Sagis, L. (2024). Interfacial moduli at large strains and stability of emulsions stabilised by plant proteins at high bulk shear rates. *Food Hydrocolloids*, 146, Article 109248. <https://doi.org/10.1016/j.foodhyd.2023.109248>
- Kergomard, J., et al. (2021). Stability to oxidation and interfacial behavior at the air/water interface of minimally-processed versus processed walnut oil-bodies. *Food Chemistry*, 360(May). <https://doi.org/10.1016/j.foodchem.2021.129880>
- Kergomard, J., et al. (2022). Interfacial organization and phase behavior of mixed galactolipid-DPPC-phytosterol assemblies at the air-water interface and in hydrated mesophases. *Colloids and Surfaces B: Biointerfaces*, 217(April), 1–10. <https://doi.org/10.1016/j.colsurfb.2022.112646>
- Keuleyan, E., et al. (2023). Pea and lupin protein ingredients: New insights into endogenous lipids and the key effect of high-pressure homogenization on their aqueous suspensions. *Food Hydrocolloids*, 141. <https://doi.org/10.1016/j.foodhyd.2023.108671>
- Kontogiorgos, V., & Prakash, S. (2023). Adsorption kinetics and dilatational rheology of plant protein concentrates at the air- and oil-water interfaces. *Food Hydrocolloids*, 138(January), Article 108486. <https://doi.org/10.1016/j.foodhyd.2023.108486>
- Larré, C., & Gueguen, J. (1986). Large-scale purification of pea globulins. Comparison between six anion exchangers in medium-pressure liquid chromatography. *Journal of Chromatography A*, 361(C), 169–178. [https://doi.org/10.1016/S0021-9673\(01\)86904-1](https://doi.org/10.1016/S0021-9673(01)86904-1)
- Liang, H. N., & Tang, C. H. (2013). Emulsifying and interfacial properties of vicilins: Role of conformational flexibility at quaternary and/or tertiary levels. *Journal of Agricultural and Food Chemistry*, 61(46), 11140–11150. <https://doi.org/10.1021/jf403847k>
- Loveday, S. M. (2019). Food proteins: Technological, nutritional, and sustainability attributes of traditional and emerging proteins. *Annual Review of Food Science and Technology*, 10, 311–339. <https://doi.org/10.1146/annurev-food-032818-121128>
- Lucassen-Reynders, E. H. (1994). Competitive adsorption of emulsifiers. *Colloids and Surfaces A: Physicochemical and Engineering Aspects*, 91, 79–88.
- Luo, L., et al. (2022). High-pressure homogenization: A potential technique for transforming insoluble pea protein isolates into soluble aggregates. *Food Chemistry*, 397(November 2021), 9. <https://doi.org/10.1016/j.foodchem.2022.133684>
- Luo, L., et al. (2022). Impact of high-pressure homogenization on physico-chemical, structural, and rheological properties of quinoa protein isolates. *Food Structure*, 32 (February). <https://doi.org/10.1016/j.foostr.2022.100265>
- Mackie, A. R., et al. (1999). Orogenic displacement of protein from the air/water interface by competitive adsorption. *Journal of Colloid and Interface Science*, 210(1), 157–166. <https://doi.org/10.1006/jcis.1998.5941>
- Maldonado-Valderrama, J., & Patino, J. M. R. (2010). Interfacial rheology of protein-surfactant mixtures. *Current Opinion in Colloid & Interface Science*, 15(4), 271–282. <https://doi.org/10.1016/j.cocis.2009.12.004>
- McClements, D. J., & Grossmann, L. (2022). The rise of plant-based foods. In *Next-generation plant-based foods* (pp. 1–21). Springer US.
- Melchior, S., et al. (2021). High pressure homogenization shapes the techno-functionalities and digestibility of pea proteins. *Food and Bioprocess Processing*, 131, 77–85. <https://doi.org/10.1016/j.fbp.2021.10.011>
- Möhwald, H. (1990). Phospholipid and phospholipid-protein monolayers at the air/water interface. *Annual Review of Physical Chemistry*, 41(1), 441–476. <https://doi.org/10.1146/annurev.pc.41.100190.002301>
- Moll, P., et al. (2021). Impact of microfluidization on colloidal properties of insoluble pea protein fractions. *European Food Research and Technology*, 247(3), 545–554. <https://doi.org/10.1007/s00217-020-03629-2>
- Nylander, T., Hamraoui, A., & Paulsson, M. (1999). Interfacial properties of whey proteins at air/water and oil/water interfaces studied by dynamic drop tensiometry, ellipsometry and spreading kinetics. *International Journal of Food Science and Technology*, 34(5–6), 573–585. <https://doi.org/10.1046/j.1365-2621.1999.00327.x>
- Poirier, A., et al. (2021). Sunflower proteins at air-water and oil-water interfaces. *Langmuir*, 37(8), 2714–2727. <https://doi.org/10.1021/acs.langmuir.0c03441>
- Renault, A., et al. (2002). Surface rheological properties of native and S-ovalbumin are correlated with the development of an intermolecular β -sheet network at the air-water interface. *Langmuir*, 18(18), 6887–6895. <https://doi.org/10.1021/la0257586>
- Rodríguez Patino, J. M., et al. (2007). Some implications of nanoscience in food dispersion formulations containing phospholipids as emulsifiers. *Food Chemistry*, 102(2), 532–541. <https://doi.org/10.1016/j.foodchem.2006.06.010>
- Russev, S. C., Arguirov, T. V., & Gurkov, T. D. (2000). β -Casein adsorption kinetics on air-water and oil-water interfaces studied by ellipsometry. *Colloids and Surfaces B: Biointerfaces*, 19(1), 89–100. [https://doi.org/10.1016/S0927-7765\(99\)00167-8](https://doi.org/10.1016/S0927-7765(99)00167-8)
- Sagis, L., & Fischer, P. (2014). Nonlinear rheology of complex fluid-fluid interfaces. *Current Opinion in Colloid & Interface Science*, 19(6), 520–529. <https://doi.org/10.1016/j.cocis.2014.09.003>
- Sagis, L., Humblet-Hua, K. N. P., & Van Kempen, S. E. H. J. (2014). Nonlinear stress deformation behavior of interfaces stabilized by food-based ingredients. *Journal of Physics: Condensed Matter*, 26(46). <https://doi.org/10.1088/0953-8984/26/46/464105>
- Sagis, L., & Scholten, E. (2014). Complex interfaces in food: Structure and mechanical properties. *Trends in Food Science and Technology*, 37(1), 59–71. <https://doi.org/10.1016/j.tifs.2014.02.009>
- Sagis, L., & Yang, J. (2022). Protein-stabilized interfaces in multiphase food: Comparing structure-function relations of plant-based and animal-based proteins. *Current Opinion in Food Science*, 43(November), 53–60. <https://doi.org/10.1016/j.cofs.2021.11.003>
- Saricaoglu, F. T. (2020). Application of high-pressure homogenization (HPH) to modify functional, structural and rheological properties of lentil (Lens culinaris) proteins. *International Journal of Biological Macromolecules*, 144, 760–769. <https://doi.org/10.1016/j.ijbiomac.2019.11.034>
- Schmitt, C., et al. (2021). Plant proteins and their colloidal state. *Current Opinion in Colloid & Interface Science*, 56, Article 101510. <https://doi.org/10.1016/j.cocis.2021.101510>
- Shen, Q., Li, J., et al. (2023). Linear and nonlinear interface rheological behaviors and structural properties of pea protein (vicilin, legumin, albumin). *Food Hydrocolloids*, 139(January), Article 108500. <https://doi.org/10.1016/j.foodhyd.2023.108500>
- Shen, Q., Luo, Y., et al. (2023a). Nonlinear rheological behavior and quantitative proteomic analysis of pea protein isolates at the air-water interface. *Food Hydrocolloids*, 135(June 2022), Article 108115. <https://doi.org/10.1016/j.foodhyd.2022.108115>
- Shen, Q., Zheng, W., et al. (2023b). Quantitative analysis and interfacial properties of mixed pea protein isolate-phospholipid adsorption layer. *International Journal of Biological Macromolecules*, 232(October 2022), Article 123487. <https://doi.org/10.1016/j.ijbiomac.2023.123487>
- Sridharan, S., et al. (2020). On the emulsifying properties of self-assembled pea protein particles. *Langmuir*, 36(41), 12221–12229. <https://doi.org/10.1021/acs.langmuir.0c01955>
- Vasilakis, K., & Dostakakis, G. (1999). The rheology of lupin seed (Lupinus albus ssp. graecus) protein isolate films at the corn oil-water interface. *Colloids and Surfaces B: Biointerfaces*, 12(3–6), 331–337. [https://doi.org/10.1016/S0927-7765\(98\)00087-3](https://doi.org/10.1016/S0927-7765(98)00087-3)
- Vié, V., et al. (1998). Distribution of ganglioside GM1 between two-component, two-phase phosphatidylcholine monolayers. *Langmuir*, 14(16), 4574–4583. <https://doi.org/10.1021/la980203p>
- Walstra, P. (2003). *Physical chemistry of foods*. CRC Press.
- Waninge, R., et al. (2005). Competitive adsorption between β -casein or β -lactoglobulin and model milk membrane lipids at oil-water interface. *Journal of Agricultural and Food Chemistry*, 53(3), 716–724. <https://doi.org/10.1021/jf049267y>
- Weiss, J. (2005). Key concepts of interfacial properties in food chemistry. *Handbook of Food Analytical Chemistry*, 1–2, 609–630. <https://doi.org/10.1002/0471709085.ch14>
- Wilde, P. J. (2000). Interfaces: Their role in foam and emulsion behaviour. *Current Opinion in Colloid & Interface Science*, 5(3–4), 176–181. [https://doi.org/10.1016/S1359-0294\(00\)00056-X](https://doi.org/10.1016/S1359-0294(00)00056-X)
- Wilde, P., et al. (2004). Proteins and emulsifiers at liquid interfaces. *Advances in Colloid and Interface Science*, 108–109, 63–71. <https://doi.org/10.1016/j.cis.2003.10.011>
- Yang, J., et al. (2018). Effects of high pressure homogenization on faba bean protein aggregation in relation to solubility and interfacial properties. *Food Hydrocolloids*, 83 (May), 275–286. <https://doi.org/10.1016/j.foodhyd.2018.05.020>
- Yang, et al. (2021). Foams and air-water interfaces stabilised by mildly purified rapeseed proteins after defatting. *Food Hydrocolloids*, 112(August 2020), Article 106270. <https://doi.org/10.1016/j.foodhyd.2020.106270>
- Yang, et al. (2022). The impact of heating and freeze or spray drying on the interface and foam stabilising properties of pea protein extracts: Explained by aggregation and protein composition. *Food Hydrocolloids*, 133(107913), 12. <https://doi.org/10.1016/j.foodhyd.2022.107913>
- Yang, et al. (2023). Surface dilatational and foaming properties of whey protein and escin mixtures. *Food Hydrocolloids*, 144(February). <https://doi.org/10.1016/j.foodhyd.2023.108941>
- Yang, & Sagis, L. (2021). Interfacial behavior of plant proteins — novel sources and extraction methods. *Current Opinion in Colloid & Interface Science*, 56(August), Article 101499. <https://doi.org/10.1016/j.cocis.2021.101499>
- Zielbauer, B. I., et al. (2018). Soybean oleosomes studied by small angle neutron scattering (SANS). *Journal of Colloid and Interface Science*, 529, 197–204. <https://doi.org/10.1016/j.jcis.2018.05.080>